© 2014. Published by The Company of Biologists Ltd | Development (2014) 141, 909-917 doi:10.1242/dev.103093

RESEARCH ARTICLE

TGFβ regulates epithelial-mesenchymal interactions through WNT signaling activity to control muscle development in the soft palate

Jun-ichi Iwata[1,2], Akiko Suzuki[1], Toshiaki Yokota[1], Thach-Vu Ho[1], Richard Pelikan[1], Mark Urata[1,3], Pedro A. Sanchez-Lara[1,4,5] and Yang Chai[1,*]

ABSTRACT

Clefting of the soft palate occurs as a congenital defect in humans and adversely affects the physiological function of the palate. However, the molecular and cellular mechanism of clefting of the soft palate remains unclear because few animal models exhibit an isolated cleft in the soft palate. Using three-dimensional microCT images and histological reconstruction, we found that loss of TGFβ signaling in the palatal epithelium led to soft palate muscle defects in *Tgfbr2*$^{fl/fl}$*;K14-Cre* mice. Specifically, muscle mass was decreased in the soft palates of *Tgfbr2* mutant mice, following defects in cell proliferation and differentiation. Gene expression of Dickkopf (*Dkk1* and *Dkk4*), negative regulators of WNT–β-catenin signaling, is upregulated in the soft palate of *Tgfbr2*$^{fl/fl}$*;K14-Cre* mice, and WNT–β-catenin signaling is disrupted in the palatal mesenchyme. Importantly, blocking the function of DKK1 and DKK4 rescued the cell proliferation and differentiation defects in the soft palate of *Tgfbr2*$^{fl/fl}$*;K14-Cre* mice. Thus, our findings indicate that loss of TGFβ signaling in epithelial cells compromises activation of WNT signaling and proper muscle development in the soft palate through tissue-tissue interactions, resulting in a cleft soft palate. This information has important implications for prevention and non-surgical correction of cleft soft palate.

KEY WORDS: Cleft soft palate, TGFβ, Epithelial-mesenchymal interactions, Mouse

INTRODUCTION

The soft palate plays important roles in swallowing, speech, hearing, middle-ear ventilation and respiration (Back et al., 2004; Evans et al., 2010; Marsh, 1991). Despite the important physiological functions of the soft palate, we know very little about the mechanisms that regulate mammalian soft palate development (Bush and Jiang, 2012; Chai and Maxson, 2006). A failure of soft palate development results in a cleft soft palate and a risk of speech problems, middle ear disease and swallowing difficulties (Carvajal Monroy et al., 2012; Precious and Delaire, 1993).

The fleshy soft palate, which makes up approximately the posterior one-third of the secondary palate, is composed of muscles, whereas the anterior two-thirds consists of the bony hard palate (Hilliard et al., 2005; Iwata et al., 2011). Clinically, individuals with a cleft in the soft palate exhibit mis-orientation and delayed development of the soft palate muscles (Cohen et al., 1994). Even after surgical correction of the cleft soft palate and reconstruction of the muscle sling, there are often functional defects in the muscles (Flores et al., 2010; van der Sloot, 2003). Therefore, patients with a defect in the soft palate need long-term therapy and additional surgical corrections after the initial surgical repair for optimal function and normal speech development (Dworkin et al., 2004; Perry, 2011).

There are five muscles in the soft palate: the tensor veli palatini (TVP), the levator veli palatini (LVP), the palatoglossus, the palatopharyngeus and the musculus uvulae (Evans et al., 2010). Their formation, like that of limb and other craniofacial muscles, is controlled by regulatory processes distinct from those governing axial muscle formation (Grenier et al., 2009). The anatomical configuration of the soft palate muscles supports its unique physiological function. Surgical repair of cleft soft palate focuses on the LVP, which is the largest muscle in the soft palate and functions in its elevation (Evans et al., 2010). The LVP may become severely atrophic because of reduced function, and often is only half as thick in cleft soft palate patients as in healthy newborns. The other muscles in the soft palate have not been well studied.

Non-cell-autonomous activation of myogenesis in different regions of the embryo is controlled by a series of complex growth factor networks and niches that ultimately result in the expression of myogenic regulatory factors within nascent and differentiating myoblasts (Snider and Tapscott, 2003). Several epithelial-specific conditional knockout mice, such as *Shh*$^{c/n}$*;K14-Cre* and *Catnb*$^{fl/fl}$*;K14-Cre*, exhibit complete cleft palate and a cell proliferation defect in palatal mesenchymal cells, suggesting that oral epithelium-derived factors probably contribute to the cell fate determination of mesenchymal cells through tissue-tissue interactions during soft palate development (He et al., 2011; Lan and Jiang, 2009). In this study, we investigated how loss of transforming growth factor, beta receptor II (*Tgfbr2*) in the epithelium results in a cleft in the soft palate.

Transforming growth factor, beta (TGFβ; TGFβ1 – Mouse Genome Informatics) signaling plays a crucial role in craniofacial development. TGFβ transmits signals through TGFβ type I and type II receptors that phosphorylate SMAD2 and SMAD3, followed by the formation of transcriptional complexes with SMAD4 and translocation into the nucleus (Massagué and Chen, 2000). In addition, SMAD-independent pathways transduce TGFβ signals in some physiological and pathological conditions (Derynck and Zhang, 2003; Iwata et al., 2012; Xu et al., 2008). TGFβ ligands

[1]Center for Craniofacial Molecular Biology, Ostrow School of Dentistry, University of Southern California, Los Angeles, CA 90033, USA. [2]Center for Craniofacial Research, Department of Diagnostic and Biomedical Sciences, School of Dentistry, The University of Texas Health Science Center at Houston, TX 77054, USA. [3]Division of Plastic Surgery, Children's Hospital Los Angeles, Los Angeles, CA 90027, USA. [4]Department of Pediatrics, Keck School of Medicine, University of Southern California, Los Angeles, CA 90027, USA. [5]Division of Medical Genetics, Children's Hospital Los Angeles, Los Angeles, CA 90027, USA.

*Author for correspondence (ychai@usc.edu)

Received 26 August 2013; Accepted 4 December 2013

Development (2014) doi:10.1242/dev.103093

target a variety of genes in a developmental stage-dependent and cell-type-specific manner (Chai and Maxson, 2006; Iwata et al., 2011). Mice with loss of *Tgfbr2* in epithelial cells (*Tgfbr2*$^{fl/fl}$*;K14-Cre*) exhibit both submucous cleft palate and cleft soft palate. Our previous studies showed that TGFβ signaling regulates gene expression of *Irf6* and the fate of the medial edge epithelium (MEE) during palatal fusion in mice (Xu et al., 2006). Interestingly, overexpression of *Irf6* fails to rescue cleft soft palate in *Tgfbr2*$^{fl/fl}$*;K14-Cre* mice although it rescues submucous cleft palate and eliminates MEE persistence, suggesting that TGFβ may regulate the disappearance of the MEE through a different signaling network than the one it uses to control soft palate muscle development (Iwata et al., 2013a). However, it remains unknown how loss of TGFβ signaling in epithelial cells causes cleft soft palate and how mesoderm-derived muscle cells are affected.

In this study, we investigated the genetic basis of muscle formation and the cellular mechanism that controls muscle development in the soft palate during embryogenesis. We show that epithelial-specific loss of *Tgfbr2* results in cleft soft palate, compromised WNT signaling due to upregulated Dickkopf-related proteins 1 and 4 (DKK1 and DKK4), and muscle deformities in the soft palate of *Tgfbr2*$^{fl/fl}$*;K14-Cre* mice. Treatment with neutralizing antibodies for DKK1 and DKK4 rescued the mesenchymal cell proliferation and muscle development defects in an *ex vivo* organ culture system. Thus, our data indicate that impaired epithelial-mesenchymal communication contributes to the pathology of cleft soft palate.

RESULTS

Muscle deformation in the soft palate of *Tgfbr2*$^{fl/fl}$*;K14-Cre* mice

Loss of TGFβ signaling in the epithelium of *Tgfbr2*$^{fl/fl}$*;K14-Cre* mice resulted in cleft soft palate with a phenotype penetrance of 100% (Fig. 1A,B). We performed three-dimensional (3D) microCT imaging analysis to examine muscle formation in the soft palate and found that the TVP and LVP muscles were reduced in volume in newborn *Tgfbr2*$^{fl/fl}$*;K14-Cre* mice compared with wild-type littermate controls (Fig. 1C-J; supplementary material Fig. S1). In addition, we generated 3D histological images of the soft palate of *Tgfbr2*$^{fl/fl}$*;K14-Cre* and wild-type control mice (Fig. 1K-P). The TVP and LVP muscles in *Tgfbr2*$^{fl/fl}$*;K14-Cre* mice were smaller than those in wild-type controls. We concluded from these results that the development of the TVP and LVP are compromised in newborn *Tgfbr2*$^{fl/fl}$*;K14-Cre* mice as the result of loss of TGFβ signaling in the palatal epithelium.

Next, we investigated the time course of muscle development in the soft palate from embryonic day (E)14.5 to E18.5 (Fig. 2A-H). Although we first detected myofibers in the soft palate of both *Tgfbr2*$^{fl/fl}$*;K14-Cre* and wild-type control mice at E15.5, the total volume of the muscle in the soft palate was reduced in *Tgfbr2*$^{fl/fl}$*;K14-Cre* mice compared with wild-type control mice. At E15.5 and later embryonic stages, *Tgfbr2*$^{fl/fl}$*;K14-Cre* mice exhibited a cleft in the soft palate, consistent with the reduction of muscle volume in the soft palate (Fig. 2I-R; supplementary material Fig.

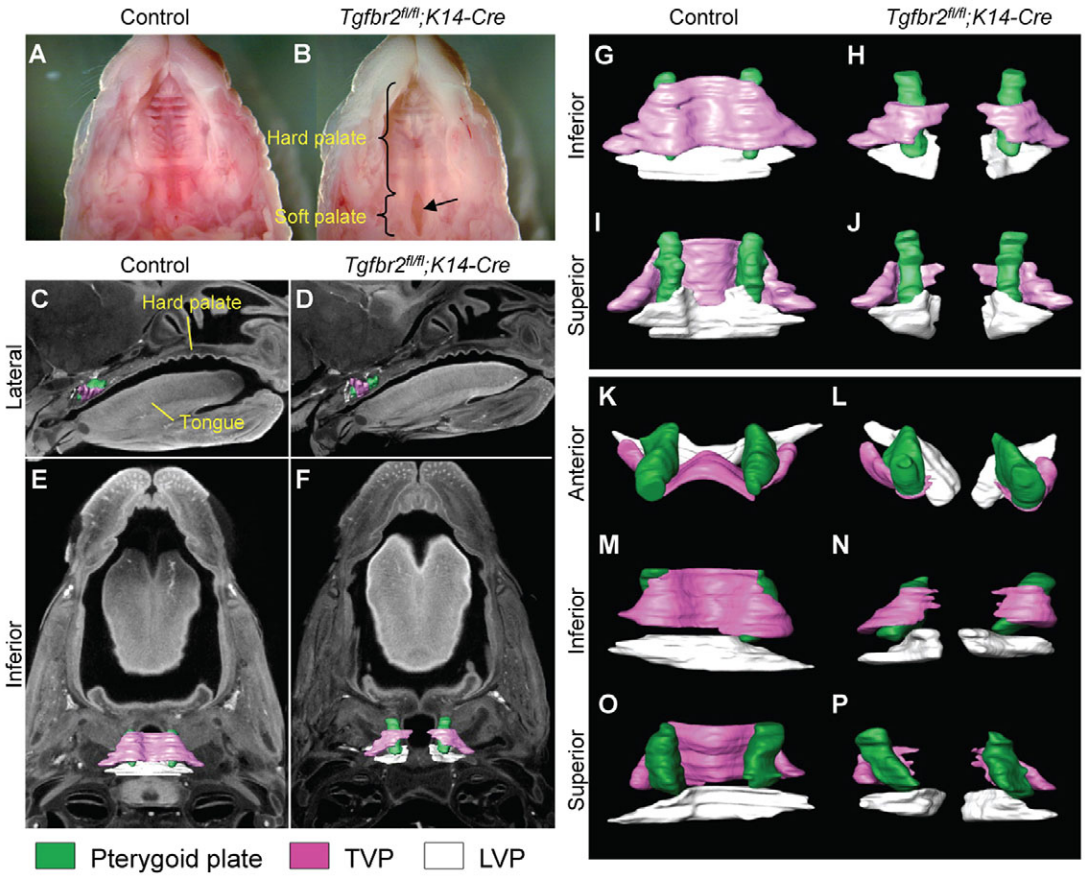

Fig. 1. Epithelial-specific loss of *Tgfbr2* in mice results in muscle mass reduction and cleft soft palate. (A,B) Macroscopic appearance of palates of newborn *Tgfbr2*$^{fl/fl}$ control and *Tgfbr2*$^{fl/fl}$*;K14-Cre* mice. Arrow indicates cleft soft palate. (C-J) 3D reconstruction of palates from microCT images of E18.5 *Tgfbr2*$^{fl/fl}$ control (C,E,G,I) and *Tgfbr2*$^{fl/fl}$*;K14-Cre* mice (D,F,H,J). Pterygoid plate (green); TVP (tensor veli palatini, pink); LVP (levator veli palatini, white). (K-P) 3D reconstruction of palates from histological sections of E18.5 *Tgfbr2*$^{fl/fl}$ control (K,M,O) and *Tgfbr2*$^{fl/fl}$*;K14-Cre* mice (L,N,P). Pterygoid plate (green); TVP (pink); LVP (white).

Development (2014) doi:10.1242/dev.103093

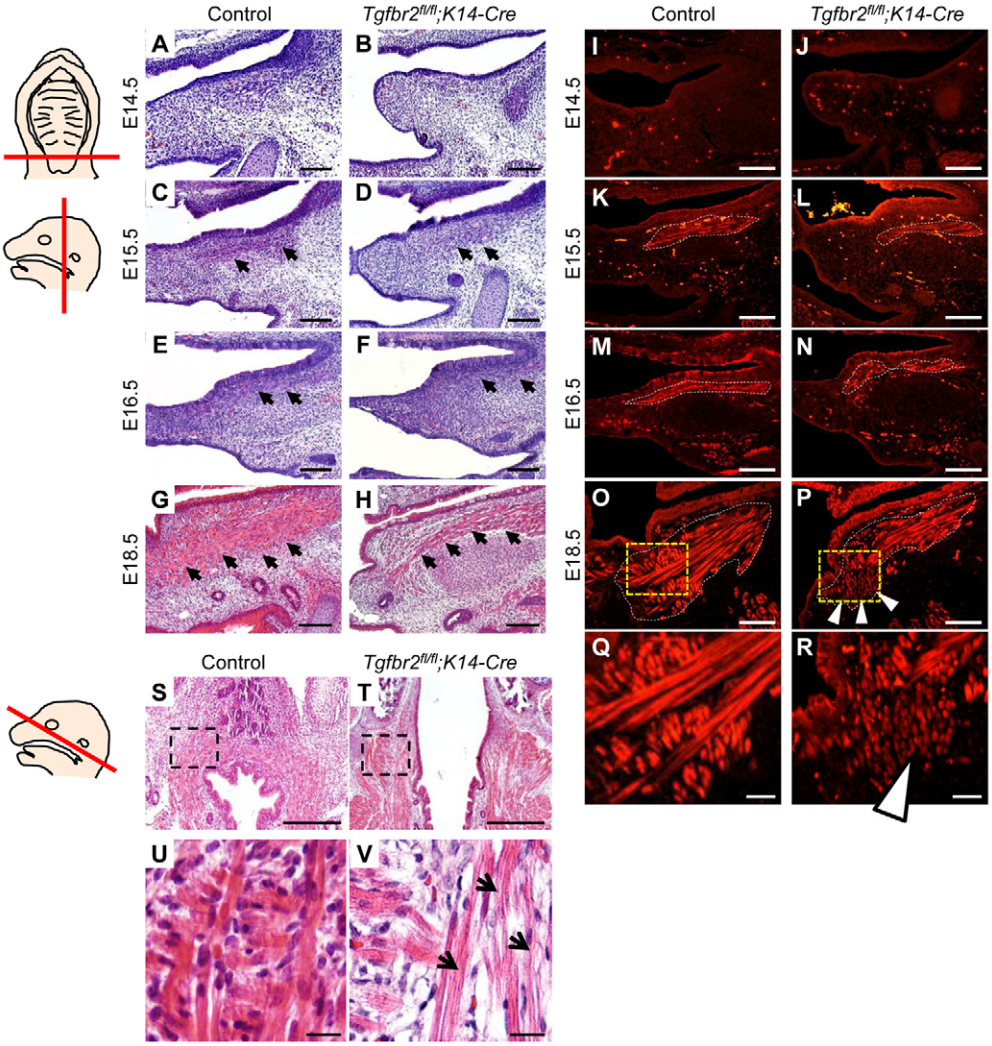

Fig. 2. Reduction of muscle mass in *Tgfbr2$^{fl/fl}$;K14-Cre* mice. (A-H) H&E staining of *Tgfbr2$^{fl/fl}$* control (A,C,E,G) and *Tgfbr2$^{fl/fl}$;K14-Cre* (B,D,F,H) mice at the indicated developmental stages. Red lines on the schematic drawings on the left show the position of the sections. Arrows indicate the LVP. Scale bars: 100 μm. (I-R) Immunohistochemical staining of myosin heavy chain (MyHC) in the soft palate of *Tgfbr2$^{fl/fl}$* control (I,K,M,O,Q) and *Tgfbr2$^{fl/fl}$;K14-Cre* (J,L,N,P,R) mice at the indicated developmental stages. Dotted lines indicate outline of the LVP. Arrowheads indicate altered orientation of muscle fibers. Boxed areas in O and P are enlarged in Q and R, respectively. Scale bars: 100 μm (I-P); 25 μm (Q,R). (S-V) H&E staining of E18.5 *Tgfbr2$^{fl/fl}$* control (S,U) and *Tgfbr2$^{fl/fl}$;K14-Cre* (T,V) mice. Boxed areas in S and T are enlarged in U and V, respectively. Red line on the schematic on the left indicates the position of the sections. Arrows indicate muscle atrophy. Scale bars: 100 μm (S,T); 10 μm (U,V).

S2). In addition, the muscle fibers were aligned in the anterior-posterior direction in the soft palate of *Tgfbr2$^{fl/fl}$;K14-Cre* mice, in contrast to the lateral-medial alignment in controls. Moreover, the muscles in *Tgfbr2$^{fl/fl}$;K14-Cre* mice were attached to the posterior border of the hard palate, similar to human patients with a cleft in the soft palate. We also found that muscle fibers in *Tgfbr2$^{fl/fl}$;K14-Cre* mice were thinner than in control mice, suggesting that *Tgfbr2$^{fl/fl}$;K14-Cre* mice may have a defect in the maturation of myotubes into myofibers (Fig. 2S-V). Collectively, these findings indicate that *Tgfbr2$^{fl/fl}$;K14-Cre* mice can serve as an excellent model to investigate the mechanism that regulates soft palate development and associated malformations.

To analyze the mechanism that causes cleft soft palate in *Tgfbr2$^{fl/fl}$;K14-Cre* mice, we investigated cell proliferation and apoptosis activities. We found that cell proliferation was reduced in *Tgfbr2$^{fl/fl}$;K14-Cre* mice at E14.5 and E15.5 (Fig. 3) but apoptosis was unaffected (supplementary material Fig. S3). Next, we investigated whether muscle differentiation and maturation were altered in the soft palate of *Tgfbr2$^{fl/fl}$;K14-Cre* mice. We found that myofibers were thin and disorganized, appearing wavy and lacking striation (Fig. 4A,B). The diameter of myofibers was decreased in *Tgfbr2$^{fl/fl}$;K14-Cre* mice (Fig. 4C). In addition, the percentage of centrally placed nuclei in myofibers was significantly increased ($P<0.05$) in *Tgfbr2$^{fl/fl}$;K14-Cre* mice compared with wild-type control mice (Fig. 4D-H). Taken together, our data indicate that failure of muscle cell proliferation and differentiation probably leads to muscle defects and cleft soft palate in *Tgfbr2$^{fl/fl}$;K14-Cre* mice.

Molecular mechanisms of cleft soft palate formation in *Tgfbr2$^{fl/fl}$;K14-Cre* mice

To explore the molecular mechanism of cleft soft palate formation in *Tgfbr2$^{fl/fl}$;K14-Cre* mice, we performed global gene expression analysis using soft palate tissue from *Tgfbr2$^{fl/fl}$;K14-Cre* and wild-type control mice at E15.5 (n=6 per genotype) and examined the downstream consequences of dysfunctional TGFβ signaling in epithelial cells. In this comparison, we uncovered 291 probe sets representing transcripts that were differentially expressed [≥1.5-fold, <5% false discovery rate (FDR)], 148 of them more abundant in *Tgfbr2$^{fl/fl}$;K14-Cre* mice (supplementary material Table S1) and 143 more abundant in wild-type control mice (supplementary material Table S2; see http://face.usc.edu//category/microarrays/). The genes identified were consistent with muscle defects, with significant reductions in the levels of transcripts related to the control of muscle movement, such as motoneurons, muscular metabolism and channel molecules for ion exchange (supplementary material Table S2). In order to examine how epithelial-specific deletion of *Tgfbr2* results in defects in muscle formation, we focused on the expression of genes related to growth differentiation factors as candidates for regulating tissue-tissue interactions. We found that transcript levels of *Dkk1* and *Dkk4*, which are negative regulators of WNT–β-catenin signaling,

Development (2014) doi:10.1242/dev.103093

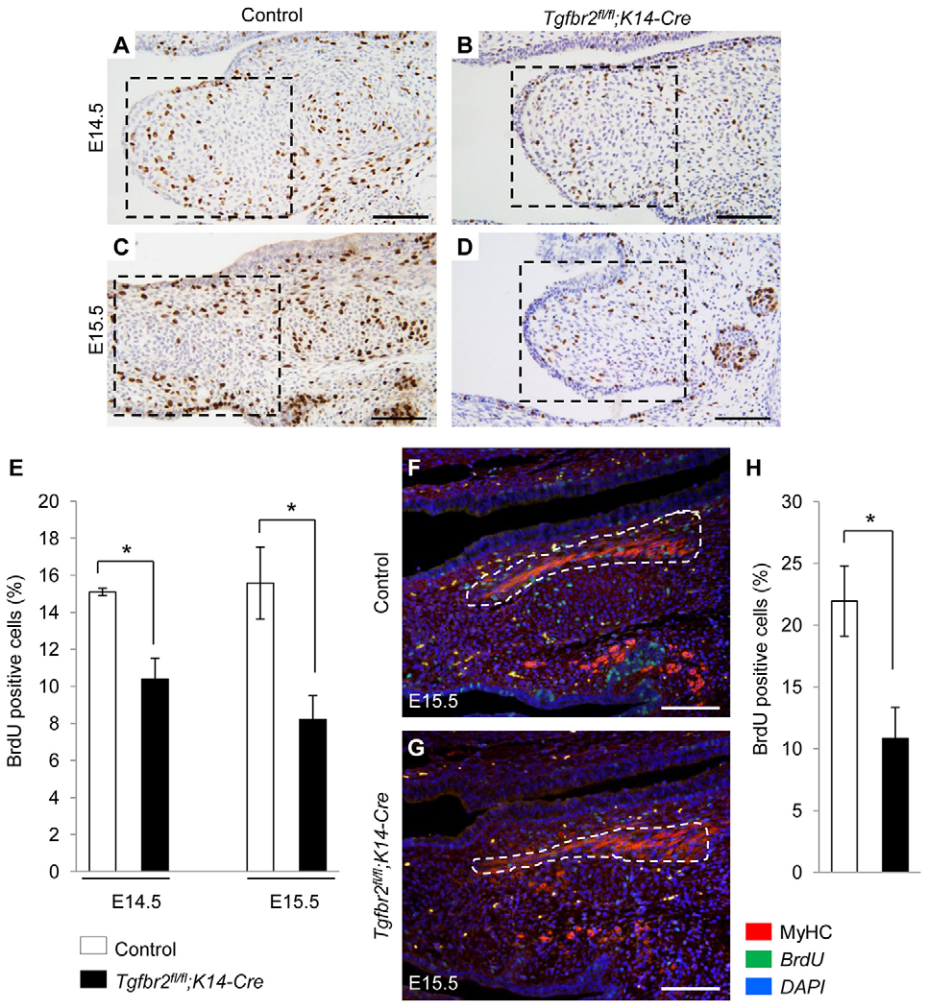

Fig. 3. Cell proliferation defect in the soft palate of *Tgfbr2$^{fl/fl}$;K14-Cre* mice. (A-D) BrdU staining (brown) of *Tgfbr2$^{fl/fl}$* control (A,C) and *Tgfbr2$^{fl/fl}$;K14-Cre* (B,D) mice at E14.5 and E15.5. Scale bars: 100 µm. (E) Quantification of the number of BrdU-labeled nuclei in the palates of *Tgfbr2$^{fl/fl}$* control (white bars) and *Tgfbr2$^{fl/fl}$;K14-Cre* (black bars) mice at E14.5 and E15.5. Three samples per genotype were analyzed. **P*<0.05; *n*=3. (F-H) Immunofluorescence images of BrdU (green) and MyHC (red) staining in the LVP of *Tgfbr2$^{fl/fl}$* control (F) and *Tgfbr2$^{fl/fl}$;K14-Cre* (G) mice at E15.5. Nuclei were counterstained with DAPI (blue). The number of BrdU-labeled nuclei is quantified in H. Three samples per genotype were analyzed. **P*<0.05. Dotted lines indicate outline of the LVP. Scale bars: 100 µm.

were significantly increased (*Dkk1*: 2.4-fold change, FDR=0.0448; *Dkk4*: 5.6-fold change, FDR=0.0103) in the soft palate of *Tgfbr2$^{fl/fl}$;K14-Cre* mice (supplementary material Table S1). We confirmed the increased gene expression levels of *Dkk1* and *Dkk4* in E15.5 *Tgfbr2$^{fl/fl}$;K14-Cre* mice by quantitative RT-PCR analysis (Fig. 5A). In order to investigate gene expression patterns of *Dkk1* and *Dkk4*, we performed whole-mount *in situ* hybridization for *Dkk1* and *Dkk4*. We detected ectopic expression in the posterior palate of E14.0 *Tgfbr2$^{fl/fl}$;K14-Cre* mice (Fig. 5B-E). We also performed section *in situ* hybridization of *Dkk1* and *Dkk4* in E15.5 *Tgfbr2$^{fl/fl}$;K14-Cre* and wild-type control mice (Fig. 5F-I). *Dkk1* and *Dkk4* gene expression was restricted to the epithelial layers and was not detectable in the palatal mesenchyme of *Tgfbr2$^{fl/fl}$;K14-Cre* mice. Next, we performed immunohistological analysis for DKK1 (Fig. 5J-Q), and found that DKK1 expression was increased in the mesenchyme of *Tgfbr2$^{fl/fl}$;K14-Cre* mice compared with wild-type control mice. DKK1 expression was detectable in the MEE in both wild-type control and *Tgfbr2$^{fl/fl}$;K14-Cre* mice at E14.5. At E15.5, the MEE started to dissociate and DKK1 expression decreased in wild-type control mice. By contrast, DKK1 expression persisted in *Tgfbr2* mutant MEE cells, and its expression was increased in the palatal mesenchyme (Fig. 5J-Q). To confirm the diffusion of DKK1 protein to the mesenchyme, we isolated palatal mesenchyme from the soft palate of E15.5 control and *Tgfbr2$^{fl/fl}$;K14-Cre* mice and performed immunoblotting analysis for DKK1 (Fig. 5R). We found that DKK1 protein was undetectable in the palatal mesenchyme from wild-type control mice. By contrast, we detected DKK1 expression in the palatal mesenchyme of *Tgfbr2$^{fl/fl}$;K14-Cre* mice. Next, to investigate whether overexpression of DKK1 affected WNT activity in *Tgfbr2$^{fl/fl}$;K14-Cre* mice, we performed immunoblotting analysis using samples from the entire E15.5 soft palate (Fig. 6A,B). In *Tgfbr2$^{fl/fl}$;K14-Cre* mice, DKK1 expression level was significantly upregulated. Moreover, we detected a decrease in the expression of the active form of β-catenin (ABC) and an increase in phosphorylated β-catenin in *Tgfbr2$^{fl/fl}$;K14-Cre* mice compared with wild-type control mice. Taken together, our data indicate that upregulated DKK1 in the palatal epithelium resulted in compromised WNT activity in the palatal mesenchyme during soft palate development.

Rescue of muscle cell proliferation and differentiation in *Tgfbr2$^{fl/fl}$;K14-Cre* soft palate

We hypothesized that inhibition of WNT signaling activity might cause defects in cell proliferation and differentiation of muscle cells, because previous studies have shown that WNT signaling is important in muscle development (Snider and Tapscot, 2003). To test this hypothesis, we cultured C2C12 cells, a mouse myoblast cell line, in proliferation or differentiation medium with or without an inhibitor for canonical WNT–β-catenin signaling (endo-IWR1). We found that endo-IWR1 suppressed cell proliferation activity in C2C12 cells (Fig. 7A). Similarly, endo-IWR1 inhibited cell proliferation activity in primary cranial neural crest (CNC)-derived MEPM cells from wild-type mice (Fig. 7B). Next, in order to test

Development (2014) doi:10.1242/dev.103093

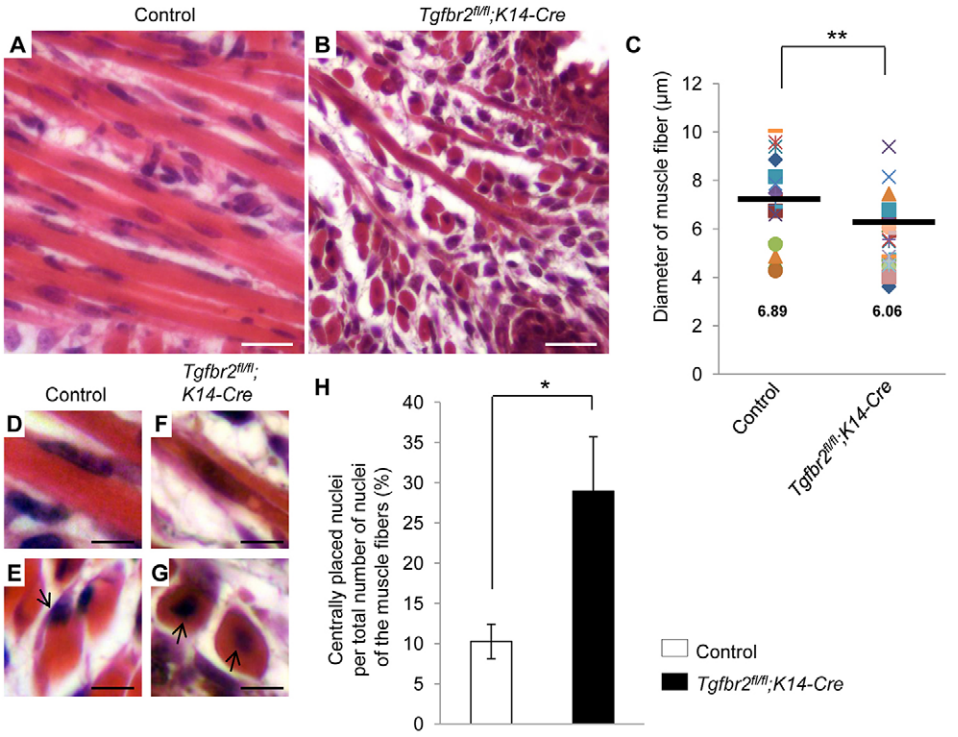

Fig. 4. Altered differentiation of myogenic cells in *Tgfbr2$^{fl/fl}$;K14-Cre* mice. (A,B) H&E staining of LVP from E18.5 *Tgfbr2$^{fl/fl}$* control (A) and *Tgfbr2$^{fl/fl}$;K14-Cre* (B) mice. Scale bars: 20 μm. (C) Quantification of the diameter of muscle fibers in the palates of E18.5 control and *Tgfbr2$^{fl/fl}$;K14-Cre* mice. Horizontal bars indicate the mean (stated below). ***P*<0.01; *n*=6. (D-G) Representative high magnification images of centrally placed nuclei in the longitudinal (D,F) or coronal (E,G) directions in A and B. Arrows indicate nuclei. Scale bars: 10 μm. (H) Quantification of the number of centrally placed nuclei out of the total number of nuclei in the muscle fibers of E18.5 control (white bar) and *Tgfbr2$^{fl/fl}$;K14-Cre* (black bar) palates. Three samples per genotype were analyzed. **P*<0.05.

whether WNT–β-catenin signaling is crucial for muscle differentiation, we cultured C2C12 cells in differentiation medium for 0, 3 or 5 days. We found that endo-IWR1 inhibited muscle differentiation in C2C12 cells (Fig. 7C-H). Moreover, we cultured wild-type palatal explants with endo-IWR1 for 1 or 3 days (Fig. 8A-J). Strikingly, wild-type palates treated with endo-IWR1 in an *ex vivo* organ culture system (Fig. 8B,E,H) mimicked the cell proliferation and differentiation defects in *Tgfbr2$^{fl/fl}$;K14-Cre* palates (Fig. 8C,F,I), whereas these activities were not affected after treatment with vehicle (Fig. 8A,D,G). Thus, our data indicate that WNT signaling is crucial for soft palate muscle development.

We hypothesized that reduction of DKK1 and DKK4 would rescue the defective cell proliferation and muscle differentiation activities in *Tgfbr2$^{fl/fl}$;K14-Cre* mice. To test this hypothesis, we treated palatal explants from *Tgfbr2$^{fl/fl}$;K14-Cre* mice with neutralizing antibodies (NAb) for DKK1 and DKK4 (Fig. 9A-J). We found that treatment with NAb for DKK1 and DKK4 could rescue the cell proliferation defect in the mesenchyme of *Tgfbr2$^{fl/fl}$;K14-Cre* palates (Fig. 9A-C,J). Similarly, treatment with NAb for DKK1 and DKK4 could rescue both muscle cell proliferation and differentiation defects in *Tgfbr2$^{fl/fl}$;K14-Cre* palates in an *ex vivo* organ culture system (Fig. 9D-J). Collectively, our findings indicate that inhibition of WNT signaling through elevated DKK1 and DKK4 expression is responsible for the failure of soft palate development and the muscle defects in *Tgfbr2$^{fl/fl}$;K14-Cre* mice (Fig. 9K).

DISCUSSION

Our mouse model for cleft soft palate, *Tgfbr2$^{fl/fl}$;K14-Cre*, suggests that specific regulators, such as growth factors, from epithelial cells may control the fate and orientation of muscle cells during palatogenesis. Importantly, this mutant mouse model mimics the phenotype of human individuals with cleft soft palate. Using the mouse model, we explored how loss of TGFβ signaling in epithelial cells results in a failure of muscle development and found that TGFβ-controlled WNT–β-catenin signaling activity is crucial for muscle formation. Previous studies indicated that DKK1 and DKK4 can inhibit WNT–β-catenin signaling (Kawano and Kypta, 2003; Nie et al., 2005; Semënov et al., 2001). *Dkk1* knockout mice exhibit severe craniofacial deformities and embryonic lethality before palatal development (Mukhopadhyay et al., 2001). Mice lacking β-catenin in CNC-derived cells (*Catnb$^{fl/fl}$;Wnt1-Cre*) exhibit severe craniofacial deformities (Brault et al., 2001), and *Wnt9b* knockout mice exhibit cleft palate (Jin et al., 2012). Thus, WNT signaling is involved in craniofacial development. Loss of WNT–β-catenin signaling results in downregulation of TGFβ, whereas expression of stabilized β-catenin in the palatal epithelium causes ectopic *Tgfb3* expression and fusion of the palatal shelf and mandible (He et al., 2011). Our study clearly shows that TGFβ signaling also affects WNT signaling activity through DKK1 and DKK4. This feedback between TGFβ and WNT signaling may be crucial for maintaining normal growth factor signaling during craniofacial development.

Tgfbr2$^{fl/fl}$;K14-Cre mice exhibit both persistence of the MEE in the hard palate (submucous cleft palate) and a cleft in the soft palate (cleft soft palate). Our previous studies showed that TGFβ signaling regulates *Irf6* gene expression and the fate of the MEE, and overexpression of *Irf6* rescues MEE disappearance although it fails to rescue the cleft in the soft palate in *Tgfbr2$^{fl/fl}$;K14-Cre* mice, indicating that the molecular mechanism of soft palate development is different from that of MEE fate determination (supplementary material Fig. S4) (Iwata et al., 2013a; Xu et al., 2006). *Irf6* is only expressed in palatal epithelial cells (Iwata et al., 2013a; Thomason et al., 2010). Hence, TGFβ regulated IRF6 signaling must only control the fate of MEE cells, and other TGFβ downstream targets must control other aspects of palate development. This reasoning is supported by our finding that *Dkk1* and *Dkk4* expression is specifically upregulated in the posterior palate of *Tgfbr2$^{fl/fl}$;K14-Cre* mice, resulting in compromised WNT–β-catenin signaling activity in the mesenchyme and soft palate muscle defects. These results suggest that TGFβ signaling plays a crucial role in regulating tissue-tissue interactions during palatogenesis. In order to investigate this further,

Development (2014) doi:10.1242/dev.103093

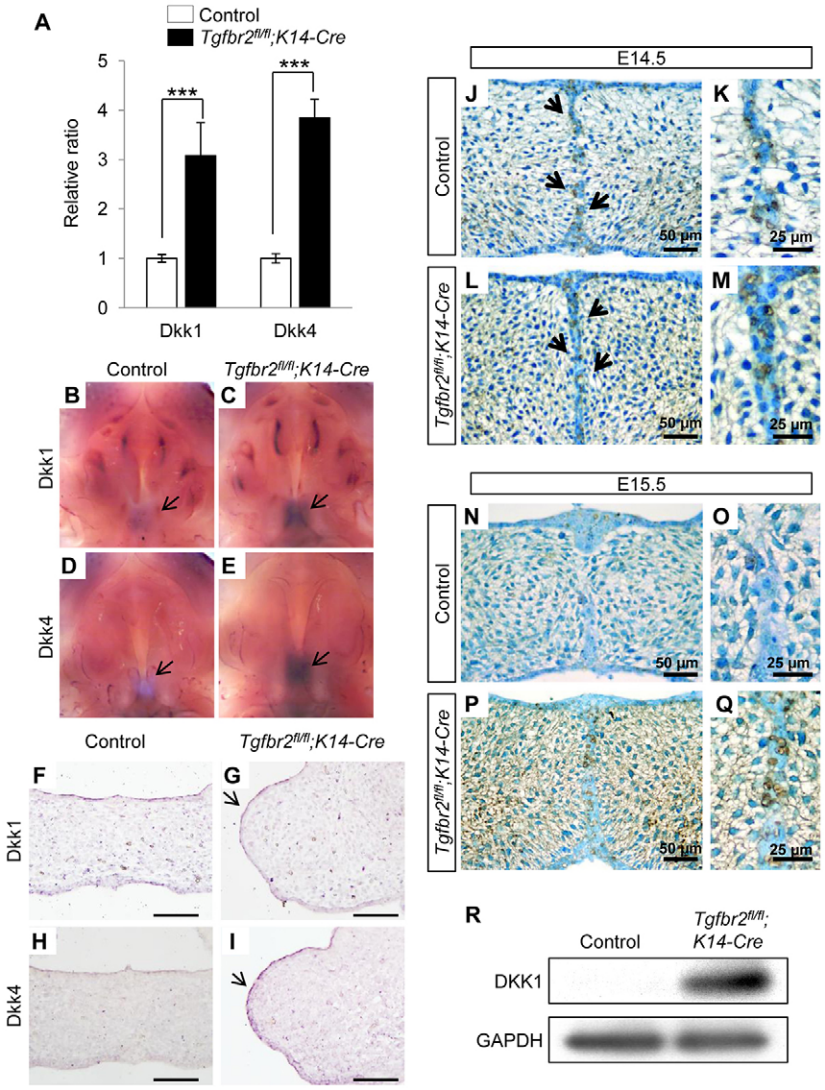

Fig. 5. Identification of molecules altered in the soft palate of *Tgfbr2*$^{fl/fl}$*;K14-Cre* mice. (A) Quantitative RT-PCR analyses of the *Dkk1* and *Dkk4* genes in the soft palates of E15.5 *Tgfbr2*$^{fl/fl}$ control (white bars) and *Tgfbr2*$^{fl/fl}$*;K14-Cre* (black bars) mice. Three samples were analyzed for each experiment. ***P<0.001. (B-E) Whole-mount *in situ* hybridization for *Dkk1* (B,C) and *Dkk4* (D,E) in E14.0 *Tgfbr2*$^{fl/fl}$ control (B,D) and *Tgfbr2*$^{fl/fl}$*;K14-Cre* (C,E) palates. Arrows indicate positive signals (purple). (F-I) Section *in situ* hybridization for *Dkk1* (F,G) and *Dkk4* (H,I) in E15.5 *Tgfbr2*$^{fl/fl}$ control (F,H) and *Tgfbr2*$^{fl/fl}$*;K14-Cre* (G,I) mice. Arrows indicate positive signals (purple). Scale bars: 100 μm. (J-Q) Immunohistochemical analysis for DKK1 in *Tgfbr2*$^{fl/fl}$ control (J,K,N,O) and *Tgfbr2*$^{fl/fl}$*;K14-Cre* (L,M,P,Q) palates at E14.5 (J-M) and E15.5 (N-Q). Arrows indicate positive signals (brown). High magnification images from J,L,N,P are shown in K,M,O,Q, respectively. Scale bars: 50 μm in J,L,N,P; 25 μm in K,M,O,Q. (R) Immunoblotting analysis of DKK1 in palatal mesenchyme of E15.5 *Tgfbr2*$^{fl/fl}$ (control) and *Tgfbr2*$^{fl/fl}$*;K14-Cre* soft palate. GAPDH was used as a loading control.

we compared gene expression profiles of the anterior and posterior palate in E15.5 wild-type mice and found that a total of 887 transcripts were differentially expressed in the soft palate. We focused on the TGFβ signaling pathway and found that TGFβ signaling mediators were differentially expressed (supplementary material Fig. S5), suggesting that TGFβ signaling is differently regulated in the anterior versus posterior palate during palate formation. This putative asymmetry is supported by our previous finding that haploinsufficiency of *Tgfbr1/Alk5* in *Tgfbr2*$^{fl/fl}$*;Wnt1-Cre* mice failed to rescue soft palate development, whereas it rescued clefting of the hard palate (Iwata et al., 2012) (our unpublished data). Our previous studies indicate that SMAD and p38 mitogen-activated protein kinase (MAPK) are functionally redundant in regulating the fate of the MEE cells (Xu et al., 2006; Iwata et al., 2013a). Therefore, gene expression of *Dkk1* and *Dkk4* may be regulated by both canonical and non-canonical TGFβ signaling. We analyzed the promoter sequences of *Dkk1* and *Dkk4* and found that the promoter regions of both genes contain SMAD-binding sites and p38 MAPK response elements (data not shown). Taken together, our findings suggest that gene expression of *Dkk1* and *Dkk4* may be regulated by TGFβ signaling in a tissue- and region-specific manner.

In addition to epithelial signals, the defects in the muscle fibers in the soft palate could also be the result of improper signaling from the cranial neural crest (CNC)-derived palatal mesenchyme. In the

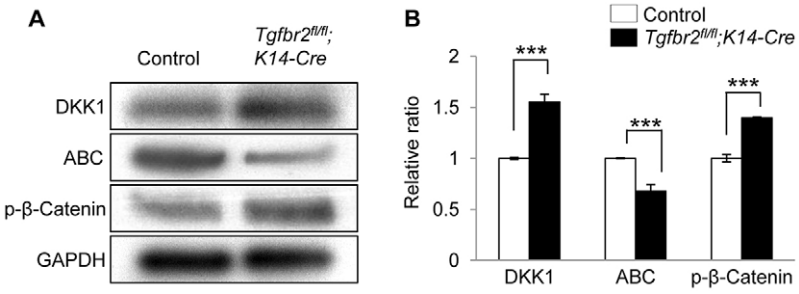

Fig. 6. Compromised WNT–β-catenin signaling activity in the soft palate of *Tgfbr2*$^{fl/fl}$*;K14-Cre* mice. (A,B) Immunoblotting analysis of DKK1, active form of β-catenin (ABC), and phosphorylated β-catenin (p-β-Catenin) in the entire soft palate of E15.5 *Tgfbr2*$^{fl/fl}$ (control) and *Tgfbr2*$^{fl/fl}$*;K14-Cre* mice. GAPDH was used as a loading control. Bar graph (B) shows the ratio of DKK1, ABC and p-β-catenin per GAPDH following quantitative densitometry analyses of immunoblots. White bars, *Tgfbr2*$^{fl/fl}$ control; black bars, *Tgfbr2*$^{fl/fl}$*;K14-Cre*. Three samples per genotype were analyzed. ***P<0.001.

Development (2014) doi:10.1242/dev.103093

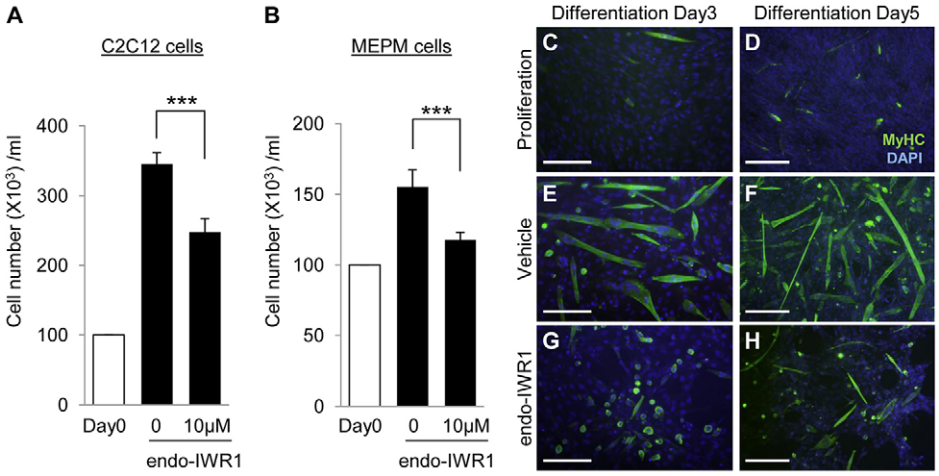

Fig. 7. Inhibition of WNT-signaling-compromised cell proliferation and differentiation activities. (A,B) Cell proliferation assays of C2C12 (A) and MEPM (B) cells after treatment with endo-IWR1 at 0 or 10 μM for 24 hours. ***P<0.001; n=6. (C-H) MyHC staining (green) with DAPI (blue) after treatment with vehicle or endo-IWR1 for the indicated number of days. Scale bars: 100 μm (C,E,G); 200 μm (D,F,H).

craniofacial region, CNC-derived cells give rise to tendons and connective tissues in the skeletal muscles, whereas these tissues are derived from the lateral mesoderm in the rest of body. CNC-specific *Tgfbr2* mutant (*Tgfbr2$^{fl/fl}$;Wnt1-Cre*) mice exhibit muscle abnormalities in the tongue (Iwata et al., 2013b) and soft palate (supplementary material Fig. S6), following defects in cell proliferation and maturation or organization. Moreover, in our microarray analyses of palates from E14.5 *Tgfbr2$^{fl/fl}$;Wnt1-Cre* mice (Iwata et al., 2012), we found that expression of genes in the WNT signaling pathway, including *Dkk2* and *Limd1*, was altered (supplementary material Figs S6, S7). Taken together, our results suggest an important positive role for CNC cells in craniofacial muscle development.

We found that elevated WNT inhibitors DKK1 and DKK4 diminished WNT–β-catenin signaling in the soft palate and adversely affected the proliferation and differentiation of myoblasts as well as the maturation of myotubes into myofibers in the palatal mesenchyme. These findings have important implications for clinical studies that aim to identify patients with cleft soft palate and families with a high risk of cleft soft palate. Moreover, this study lays the groundwork for efforts to reorient soft palate muscles and to accelerate muscle regeneration in patients with cleft soft palate. Our study of soft palate development could also be useful for understanding tissue-tissue interaction mechanisms in regulating skeletal muscle development and regeneration.

MATERIALS AND METHODS

Animals

To generate *Tgfbr2$^{fl/fl}$;K14-Cre* mice, we mated *Tgfbr2$^{fl/+}$;K14-Cre* with *Tgfbr2$^{fl/fl}$* mice. To generate *Tgfbr2$^{fl/fl}$;K14-Cre;Irf6^{Tg}* mice, we mated *Tgfbr2$^{fl/+}$;K14-Cre;Irf6^{Tg}* with *Tgfbr2$^{fl/fl}$* mice. To generate *Tgfbr2$^{fl/fl}$;Wnt1-Cre* mice, we mated T*gfbr2$^{fl/+}$;Wnt1-Cre* with *Tgfbr2$^{fl/fl}$* mice. Genotyping was performed using PCR primers as described previously (Iwata et al., 2012; Iwata et al., 2013a; Xu et al., 2006).

MicroCT analysis

MicroCT analysis was performed using a SCANCO μCT50 device at the University of Southern California Molecular Imaging Center. The microCT images were acquired with the X-ray source at 70 kVp and 114 μA. The data were collected at a resolution of 10 μm. The three-dimensional (3D) reconstruction was done with AVIZO 7.1 software (Visualization Sciences Group).

Microarray analysis

Total RNA samples (1 μg per sample) were isolated from E15.5 soft palate of control and *Tgfbr2$^{fl/fl}$;K14-Cre* mice, and converted into biotin-labeled cRNA using the GeneChip IVT Labeling Kit with Biotin-ddUTP and standard protocols recommended by Affymetrix (Santa Clara, CA, USA). Fragmented cDNA was applied to GeneChip Mouse Genome 430 2.0 Arrays (Affymetrix) containing probe sets designed to detect over 39,000 transcripts. Microarrays were hybridized, processed and scanned as previously described (Karaman et al., 2003), using the manufacturer's recommended conditions. WebArray software was used to generate scaled $\log_2$-transformed gene expression values using the RMA algorithm (Wang et al., 2009; Xia et al., 2005). Probes sets showing ≥1.5-fold differential expression with a <5% false discovery rate (FDR) were identified through liner models for microarray data (LIMMA)-based liner model statistical analysis (Smyth, 2004) and FDR calculations made using the spacings LOESS histogram (SPLOSH) method (Pounds and Cheng, 2004). All scaled gene expression scores and .cel files are available at the National Center for Biotechnology Information (NCBI) Gene Expression Omnibus (GEO) repository under the series accession number GSE46211.

Histological examination

Hematoxylin and Eosin (H&E), BrdU and immunohistochemical staining were performed as described previously (Iwata et al., 2010; Iwata et al., 2012; Iwata et al., 2013a). Antibodies used for immunohistochemistry were mouse monoclonal antibody against myosin heavy chain (MyHC; Sigma-Aldrich) and DKK1 (Santa Cruz Biotechnology). Fluorescence images were obtained using a fluorescence microscope (Model IX71, Olympus).

Quantitative RT-PCR

Total RNA was isolated from mouse soft palate dissected at E15.5 using QIAshredder and RNeasy Micro extraction kits (Qiagen), as described previously (Iwata et al., 2010). The following PCR primers were used: *Dkk1*, 5′-GAGGGGAAATTGAGGAAAGC-3′ and 5′-GGTGCACACCTG-ACCTTCTT-3′; *Dkk4*, 5′-TAGAGTTCGCAGGAGGTGTC-3′ and 5′-TGAGGTCTGTTTTCCTCTGC-3′; *Dkk2*, 5′-ACCCTTGCAGCAGTGA-TAAG-3′ and 5′-TGGCTTTGGAAGAGTAGGTG-3′; *Limd1*, 5′-CGGA-CTACTTCGGTTCCTGT-3′ and 5′-TTACAGATGACGCAGCGGAA-3′; and *Gapdh*, 5′-AACTTTGGCATTGTGGAAGG-3′ and 5′-ACACATTG-GGGGTAGGAACA-3′. A two-tailed Student's t-test was applied for statistical analysis of quantitative PCR data. A P-value ≤0.05 was considered statistically significant. For all graphs, data are means ± standard deviation (s.d.).

Immunoblotting analysis

Immunoblotting was performed as described previously (Iwata et al., 2012; Iwata et al., 2013b). Antibodies used for immunoblotting were as follows: mouse monoclonal antibodies against DKK1 (Santa Cruz Biotechnology), active form of β-catenin (ABC) and GAPDH (Millipore), and rabbit polyclonal antibody against phosphorylated β-catenin (Cell Signaling Technology).

Development (2014) doi:10.1242/dev.103093

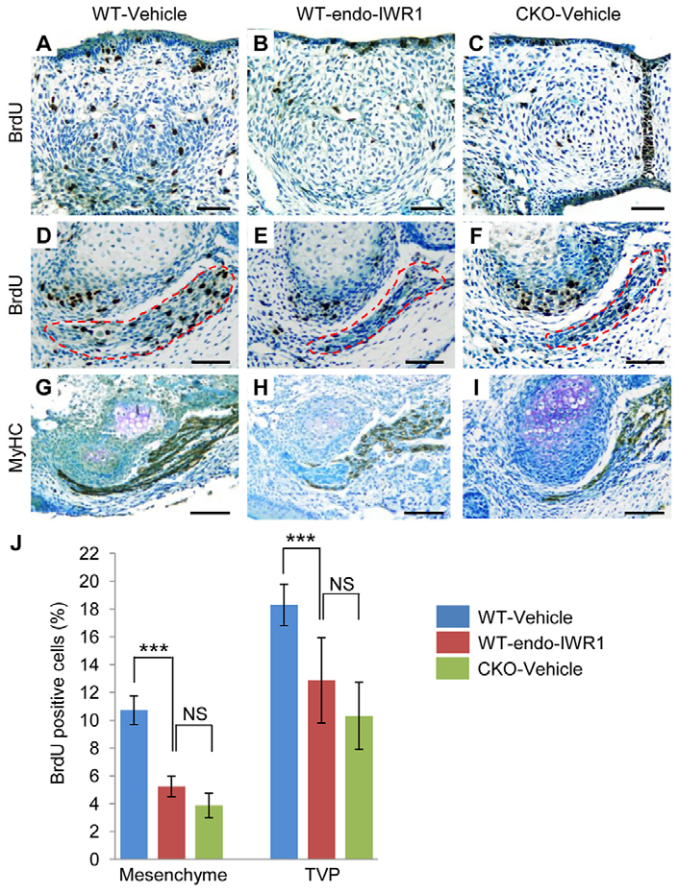

Fig. 8. Inhibition of WNT signaling causes cell proliferation and muscle differentiation defects in palatal explants. (A-C) BrdU staining after treatment with vehicle or endo-IWR1 for 1 day in palatal explants from wild-type mice (A,B) or treatment with vehicle in *Tgfbr2*$^{fl/fl}$*;K14-Cre* mice (C). Scale bars: 50 µm. (D-I) BrdU (D-F) and MyHC staining (G-I) after treatment with vehicle (D,G) or endo-IWR1 (E,H) for 3 days in palatal explants from wild-type mice (D,E,G,H) or treatment with vehicle in palatal explants from *Tgfbr2*$^{fl/fl}$*;K14-Cre* mice (F,I). Dotted lines indicate the outline of the TVP. Scale bars: 50 µm. (J) Quantification of the number of BrdU-labeled nuclei after treatment with vehicle (blue bars) or endo-IWR1 (red bars) in the mesenchyme or the TVP of wild-type palatal explants and treatment with vehicle in palatal explants from *Tgfbr2*$^{fl/fl}$*;K14-Cre* mice (green bars). Six samples per group were analyzed. ***P<0.001; NS, not significant.

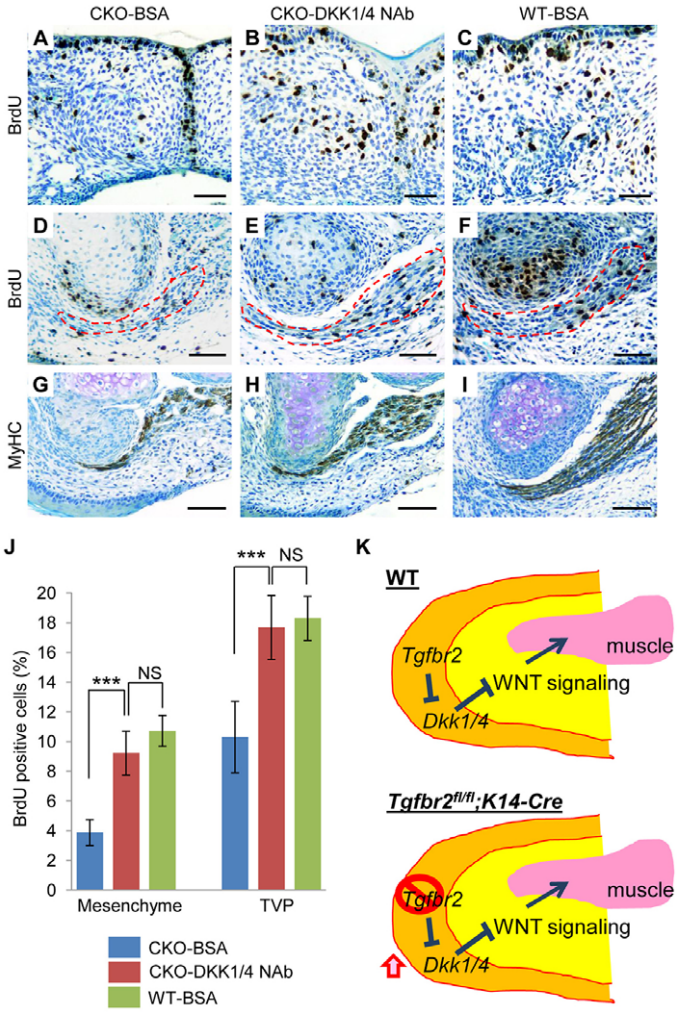

Fig. 9. Restored cell proliferation and muscle differentiation activities in the soft palate of *Tgfbr2*$^{fl/fl}$*;K14-Cre* mice. (A-C) BrdU staining after treatment with BSA (A) or neutralizing antibody (NAb) for DKK1 and DKK4 (B) for 1 day in *Tgfbr2*$^{fl/fl}$*;K14-Cre* soft palate explants and with BSA in *Tgfbr2*$^{fl/fl}$ control soft palate explants (C). Scale bars: 50 µm. (D-I) BrdU (D-F) and MyHC staining (G-I) after treatment with BSA (D,G) or NAb for DKK1 and DKK4 (E,H) for 3 days in *Tgfbr2*$^{fl/fl}$*;K14-Cre* palatal explants and with BSA in *Tgfbr2*$^{fl/fl}$ control palatal explants (F,I). Dotted lines indicate the outline of the TVP. Scale bars: 50 µm. (J) Quantification of the number of BrdU-labeled nuclei after treatment with BSA (blue bars) or DKK1/4 NAb (red bars) in the mesenchyme or the TVP of *Tgfbr2*$^{fl/fl}$*;K14-Cre* palatal explants and treatment with BSA in the wild-type palatal explants (green bars). Six samples per group were analyzed. ***P<0.001; NS, not significant. (K) Schematic depicts our model of the mechanism of soft palate development in wild-type (WT; upper panel) and *Tgfbr2*$^{fl/fl}$*;K14-Cre* mice (lower panel). Loss of *Tgfbr2* results in upregulated expression of *Dkk1* and *Dkk4* and inhibits WNT signaling in the palatal mesenchyme, resulting in muscle defects.

Palatal shelf organ culture

Timed-pregnant mice were sacrificed at E15.5. Genotyping was carried out as described above. The palatal shelves were micro-dissected and cultured in BGJb medium supplemented with penicillin, streptomycin, vitamin C and 10% fetal bovine serum. After 24 or 72 hours in culture with neutralizing antibodies (1 µg/ml each) for DKK1 and DKK4, or WNT inhibitor endo-IWR1 (50 µM; Tocris Bioscience), soft palate explants were fixed in 4% paraformaldehyde in 0.1 M phosphate buffer (pH 7.4) and processed for histological analysis as previously described (Iwata et al., 2012).

Whole-mount and section *in situ* hybridization

The probes for *Dkk1* and *Dkk4* were obtained from Dr Irma Thesleff (University of Helsinki, Finland). *In situ* hybridization was performed as described previously (Iwata et al., 2010). Several negative controls (e.g. sense probe and no probe) were run in parallel with the experimental reaction.

Cell culture

Primary mouse embryonic palatal mesenchymal (MEPM) cells were obtained from E13.5 embryos as described previously (Iwata et al., 2012). C2C12 cells (ATCC) were cultured in Dulbecco's modified Eagle's medium (DMEM) containing 10% fetal bovine serum supplemented with penicillin, streptomycin, L-glutamate, sodium pyruvate and nonessential amino acids. Cell proliferation assays were performed using a cell counting kit (Dojindo Molecular Technologies). MEPM and C2C12 cells were treated with endo-IWR1 (Tocris Bioscience) at 10 µM for 24 hours or left untreated. Myogenic differentiation was induced by culture in a monolayer in differentiation medium (DMEM supplemented with 2% donor equine serum, 1 µM insulin, penicillin, streptomycin and L-glutamate) for 3 or 5 days. Myofibers were stained with MyHC. All fluorescence images were obtained using a

fluorescence microscope (Model IX71, Olympus). Pictures were taken using MicroSuite Analytical Suite software (Olympus).

Statistical analysis

Two-tailed Student's *t*-tests were applied for statistical analysis. For all graphs, data are mean ± s.d. A *P*-value of less than 0.05 was considered statistically significant.

Acknowledgements

We thank Drs J. Mayo and B. Samuels for critical reading of the manuscript; Dr H. Moses for *Tgfbr2*$^{fl/fl}$ mice; Dr H. Slavkin for discussion; P. Bringas, Jr, O. Chaudhry, the Molecular Imaging Center and the Microarray core of CHLA for technical assistance.

Competing interests

The authors declare no competing financial interests.

Author contributions

J.I., A.S. and Y.C. designed research; J.I., A.S. and T.Y. performed experiments; T.-V.H., M.U. and P.A.S.-L. performed microCT imaging analysis; J.I. and Y.C. wrote the manuscript. R.P. performed the microarray analyses.

Funding

This work was supported by grants from the National Institute of Dental and Craniofacial Research [DE020065 and DE012711 to Y.C.]. Deposited in PMC for release after 12 months.

Supplementary material

Supplementary material available online at
http://dev.biologists.org/lookup/suppl/doi:10.1242/dev.103093/-/DC1

References

Back, G. W., Nadig, S., Uppal, S. and Coatesworth, A. P. (2004). Why do we have a uvula?: literature review and a new theory. *Clin. Otolaryngol. Allied Sci.* **29**, 689-693.

Brault, V., Moore, R., Kutsch, S., Ishibashi, M., Rowitch, D. H., McMahon, A. P., Sommer, L., Boussadia, O. and Kemler, R. (2001). Inactivation of the beta-catenin gene by Wnt1-Cre-mediated deletion results in dramatic brain malformation and failure of craniofacial development. *Development* **128**, 1253-1264.

Bush, J. O. and Jiang, R. (2012). Palatogenesis: morphogenetic and molecular mechanisms of secondary palate development. *Development* **139**, 231-243.

Carvajal Monroy, P. L., Grefte, S., Kuijpers-Jagtman, A. M., Wagener, F. A. and Von den Hoff, J. (2012). Strategies to improve regeneration of the soft palate muscles after cleft palate repair. *Tissue Eng. Part B Rev.* **18**, 468-477.

Chai, Y. and Maxson, R. E., Jr (2006). Recent advances in craniofacial morphogenesis. *Dev. Dyn.* **235**, 2353-2375.

Cohen, S. R., Chen, L. L., Burdi, A. R. and Trotman, C. A. (1994). Patterns of abnormal myogenesis in human cleft palates. *Cleft Palate Craniofac. J.* **31**, 345-350.

Derynck, R. and Zhang, Y. E. (2003). Smad-dependent and Smad-independent pathways in TGF-beta family signalling. *Nature* **425**, 577-584.

Dworkin, J. P., Marunick, M. T. and Krouse, J. H. (2004). Velopharyngeal dysfunction: speech characteristics, variable etiologies, evaluation techniques, and differential treatments. *Lang. Speech Hear. Serv. Sch.* **35**, 333-352.

Evans, A., Ackermann, B. and Driscoll, T. (2010). Functional anatomy of the soft palate applied to wind playing. *Med. Probl. Perform. Art.* **25**, 183-189.

Flores, R. L., Jones, B. L., Bernstein, J., Karnell, M., Canady, J. and Cutting, C. B. (2010). Tensor veli palatini preservation, transection, and transection with tensor tenopexy during cleft palate repair and its effects on eustachian tube function. *Plast. Reconstr. Surg.* **125**, 282-289.

Grenier, J., Teillet, M. A., Grifone, R., Kelly, R. G. and Duprez, D. (2009). Relationship between neural crest cells and cranial mesoderm during head muscle development. *PLoS ONE* **4**, e4381.

He, F., Xiong, W., Wang, Y., Li, L., Liu, C., Yamagami, T., Taketo, M. M., Zhou, C. and Chen, Y. (2011). Epithelial Wnt/β-catenin signaling regulates palatal shelf fusion through regulation of Tgfβ3 expression. *Dev. Biol.* **350**, 511-519.

Hilliard, S. A., Yu, L., Gu, S., Zhang, Z. and Chen, Y. P. (2005). Regional regulation of palatal growth and patterning along the anterior-posterior axis in mice. *J. Anat.* **207**, 655-667.

Iwata, J., Hosokawa, R., Sanchez-Lara, P. A., Urata, M., Slavkin, H. and Chai, Y. (2010). Transforming growth factor-beta regulates basal transcriptional regulatory machinery to control cell proliferation and differentiation in cranial neural crest-derived osteoprogenitor cells. *J. Biol. Chem.* **285**, 4975-4982.

Iwata, J., Parada, C. and Chai, Y. (2011). The mechanism of TGF-β signaling during palate development. *Oral Dis.* **17**, 733-744.

Iwata, J., Hacia, J. G., Suzuki, A., Sanchez-Lara, P. A., Urata, M. and Chai, Y. (2012). Modulation of noncanonical TGF-β signaling prevents cleft palate in Tgfbr2 mutant mice. *J. Clin. Invest.* **122**, 873-885.

Iwata, J., Suzuki, A., Pelikan, R. C., Ho, T. V., Sanchez-Lara, P. A., Urata, M., Dixon, M. J. and Chai, Y. (2013a). Smad4-Irf6 genetic interaction and TGFβ-mediated IRF6 signaling cascade are crucial for palatal fusion in mice. *Development* **140**, 1220-1230.

Iwata, J., Suzuki, A., Pelikan, R. C., Ho, T. V. and Chai, Y. (2013b). Noncanonical transforming growth factor β (TGFβ) signaling in cranial neural crest cells causes tongue muscle developmental defects. *J. Biol. Chem.* **288**, 29760-29770.

Jin, Y. R., Han, X. H., Taketo, M. M. and Yoon, J. K. (2012). Wnt9b-dependent FGF signaling is crucial for outgrowth of the nasal and maxillary processes during upper jaw and lip development. *Development* **139**, 1821-1830.

Karaman, M. W., Houck, M. L., Chemnick, L. G., Nagpal, S., Chawannakul, D., Sudano, D., Pike, B. L., Ho, V. V., Ryder, O. A. and Hacia, J. G. (2003). Comparative analysis of gene-expression patterns in human and African great ape cultured fibroblasts. *Genome Res.* **13**, 1619-1630.

Kawano, Y. and Kypta, R. (2003). Secreted antagonists of the Wnt signalling pathway. *J. Cell Sci.* **116**, 2627-2634.

Lan, Y. and Jiang, R. (2009). Sonic hedgehog signaling regulates reciprocal epithelial-mesenchymal interactions controlling palatal outgrowth. *Development* **136**, 1387-1396.

Marsh, J. L. (1991). Cleft palate and velopharyngeal dysfunction. *Clin. Commun. Disord.* **1**, 29-34.

Massagué, J. and Chen, Y. G. (2000). Controlling TGF-beta signaling. *Genes Dev.* **14**, 627-644.

Mukhopadhyay, M., Shtrom, S., Rodriguez-Esteban, C., Chen, L., Tsukui, T., Gomer, L., Dorward, D. W., Glinka, A., Grinberg, A., Huang, S. P. et al. (2001). Dickkopf1 is required for embryonic head induction and limb morphogenesis in the mouse. *Dev. Cell* **1**, 423-434.

Nie, X., Luukko, K., Fjeld, K., Kvinnsland, I. H. and Kettunen, P. (2005). Developmental expression of Dkk1-3 and Mmp9 and apoptosis in cranial base of mice. *J. Mol. Histol.* **36**, 419-426.

Perry, J. L. (2011). Anatomy and physiology of the velopharyngeal mechanism. *Semin. Speech Lang.* **32**, 83-92.

Pounds, S. and Cheng, C. (2004). Improving false discovery rate estimation. *Bioinformatics* **20**, 1737-1745.

Precious, D. S. and Delaire, J. (1993). Clinical observations of cleft lip and palate. *Oral Surg. Oral Med. Oral Pathol.* **75**, 141-151.

Semënov, M. V., Tamai, K., Brott, B. K., Kühl, M., Sokol, S. and He, X. (2001). Head inducer Dickkopf-1 is a ligand for Wnt coreceptor LRP6. *Curr. Biol.* **11**, 951-961.

Smyth, G. K. (2004). Linear models and empirical bayes methods for assessing differential expression in microarray experiments. *Stat. Appl. Genet. Mol. Biol.* **3**, Article3.

Snider, L. and Tapscott, S. J. (2003). Emerging parallels in the generation and regeneration of skeletal muscle. *Cell* **113**, 811-812.

Thomason, H. A., Zhou, H., Kouwenhoven, E. N., Dotto, G. P., Restivo, G., Nguyen, B. C., Little, H., Dixon, M. J., van Bokhoven, H. and Dixon, J. (2010). Cooperation between the transcription factors p63 and IRF6 is essential to prevent cleft palate in mice. *J. Clin. Invest.* **120**, 1561-1569.

van der Sloot, P. G. (2003). Hard and soft palate reconstruction. *Curr. Opin. Otolaryngol. Head Neck Surg.* **11**, 225-229.

Wang, Y., McClelland, M. and Xia, X. Q. (2009). Analyzing microarray data using WebArray. *Cold Spring Harb. Protoc.* **2009**, pdb prot5260.

Xia, X., McClelland, M. and Wang, Y. (2005). WebArray: an online platform for microarray data analysis. *BMC Bioinformatics* **6**, 306.

Xu, X., Han, J., Ito, Y., Bringas, P., Jr, Urata, M. M. and Chai, Y. (2006). Cell autonomous requirement for Tgfbr2 in the disappearance of medial edge epithelium during palatal fusion. *Dev. Biol.* **297**, 238-248.

Xu, X., Han, J., Ito, Y., Bringas, P., Jr, Deng, C. and Chai, Y. (2008). Ectodermal Smad4 and p38 MAPK are functionally redundant in mediating TGF-beta/BMP signaling during tooth and palate development. *Dev. Cell* **15**, 322-329.

SUPPLEMENTARY MATERIAL

Supplementary Figures S1 to S7

Supplementary Tables S1 and S2

Supplementary Figure Legends

Fig. S1. MicroCT imaging analysis in *Tgfbr2$^{fl/fl}$;K14-Cre* mice. (**A-L**) MicroCT images from E18.5 *Tgfbr2$^{fl/fl}$* control (A-F) and *Tgfbr2$^{fl/fl}$;K14-Cre* (G-L) mice, arranged from the anterior to posterior. Images of (B,D,F,H,J,L) are enlarged from (A,C,E,G,J,K), respectively. Yellow arrows indicate cleft palate. Scale bars, 1.0 mm in (A,C,E,G,J,K); 250 μm in (B,D,F,H,J,L).

Fig. S2. Comparison of palate development in *Tgfbr2$^{fl/fl}$* control and *Tgfbr2$^{fl/fl}$;K14-Cre* mice. (**A-Y**) Coronal images of H&E staining from the anterior to posterior of *Tgfbr2$^{fl/fl}$* control (A-C,G-I,M-O,S-U) and *Tgfbr2$^{fl/fl}$;K14-Cre* (D-F,J-L,P-R,V-X) mice at the indicated developmental stages. Red lines on the schematic drawings (Y) show the position of the sections. Scale bars, 200 μm.

Fig. S3. Apoptotic activity is not altered in *Tgfbr2$^{fl/fl}$;K14-Cre* mice. (**A-F**) H&E staining (A, B), BrdU staining (C, D), and immunofluorescent staining with MyHC (green) and BrdU (red) (E, F) of *Tgfbr2$^{fl/fl}$* control (A,C,E) and *Tgfbr2$^{fl/fl}$;K14-Cre* (B,D,F) mice at E15.5. Dotted lines indicate outline of the TVP. Scale bars, 50 μm (**G**) Quantification of the number of BrdU-labeled nuclei in the TVP of E15.5 *Tgfbr2$^{fl/fl}$* control (white bar) and *Tgfbr2$^{fl/fl}$;K14-Cre* (black bar) mice. Three samples per genotype were analyzed. *, $p<0.05$. (**H-M**) TUNEL assay of the soft palate of *Tgfbr2$^{fl/fl}$* control (H,I,L) and *Tgfbr2$^{fl/fl}$;K14-Cre* (J,K,M) mice at E15.5 (H-K) and E16.5 (L,M). Insets (I,K) show higher magnification of (H,K), respectively. Scale bars, 100 μm

Fig. S4. Cleft soft palate in *Tgfbr2$^{fl/fl}$;K14-Cre;Irf6^{Tg}* mice. (**A-L**) H&E staining of *Tgfbr2$^{fl/fl}$* control (A,D,G,J), *Tgfbr2$^{fl/fl}$;K14-Cre* (B,E,H,K), and *Tgfbr2$^{fl/fl}$;K14-Cre;Irf6^{Tg}* (C,F,I,L) mice at E15.5 and E18.5. Scale bars, 200 μm. (**M**) Quantitative RT-PCR analyses of *Dkk1* and *Dkk4* in the palates of E15.5 *Tgfbr2$^{fl/fl}$* control (blue bars), *Tgfbr2$^{fl/fl}$;K14-Cre* (red bars), and *Tgfbr2$^{fl/fl}$;K14-Cre;Irf6^{Tg}* (green bars) mice. Three samples were analyzed for each experiment. ***, $p<0.001$; *, $p<0.05$; NS, not significant.

Fig. S5. Heat map image of TGFβ signaling pathway in the anterior versus posterior palate of E15.5 wild type mice. Anterior and posterior portions of the secondary palate from E15.5 wild type mice. Six samples per group were analyzed.

Fig. S6. Soft palate development in *Tgfbr2$^{fl/fl}$;Wnt1-Cre* mice. (**A,B**) Oral view of E18.5 *Tgfbr2$^{fl/fl}$* control (A) and *Tgfbr2$^{fl/fl}$;Wnt1-Cre* (B) mice. Yellow dotted lines indicate the pterygoid plate. Blue dotted lines indicate the end of the soft palate. (**C-J**) H&E staining of E18.5 *Tgfbr2$^{fl/fl}$* control (C,D,G,H), *Tgfbr2$^{fl/fl}$;Wnt1-Cre* (E,F,I,J) mice. Boxed areas in (C,E,G,I) are enlarged in (D,F,H,J), respectively. Scale bars, 500 μm in (C,E,G,I); 50 μm in (D,F,H,J). Ptr, pterygoid plate. (**K**) Quantitative RT-PCR analyses of *Dkk2* and *Limd1* in the palates of E15.5 *Tgfbr2$^{fl/fl}$* control (white bars) and *Tgfbr2$^{fl/fl}$;Wnt1-Cre* (black bars) mice. Three samples were analyzed for each experiment. ***, $p<0.001$; *, $p<0.05$.

Fig. S7. Heat map image of canonical WNT signaling pathway in *Tgfbr2$^{fl/fl}$;Wnt1-Cre* palate. Palatal shelves from E14.5 *Tgfbr2$^{fl/fl}$* control and *Tgfbr2$^{fl/fl}$;Wnt1-Cre* mice. Five samples per genotype were analyzed.

Control

Tgfbr2$^{fl/fl}$;*K14-Cre*

Fig. S1

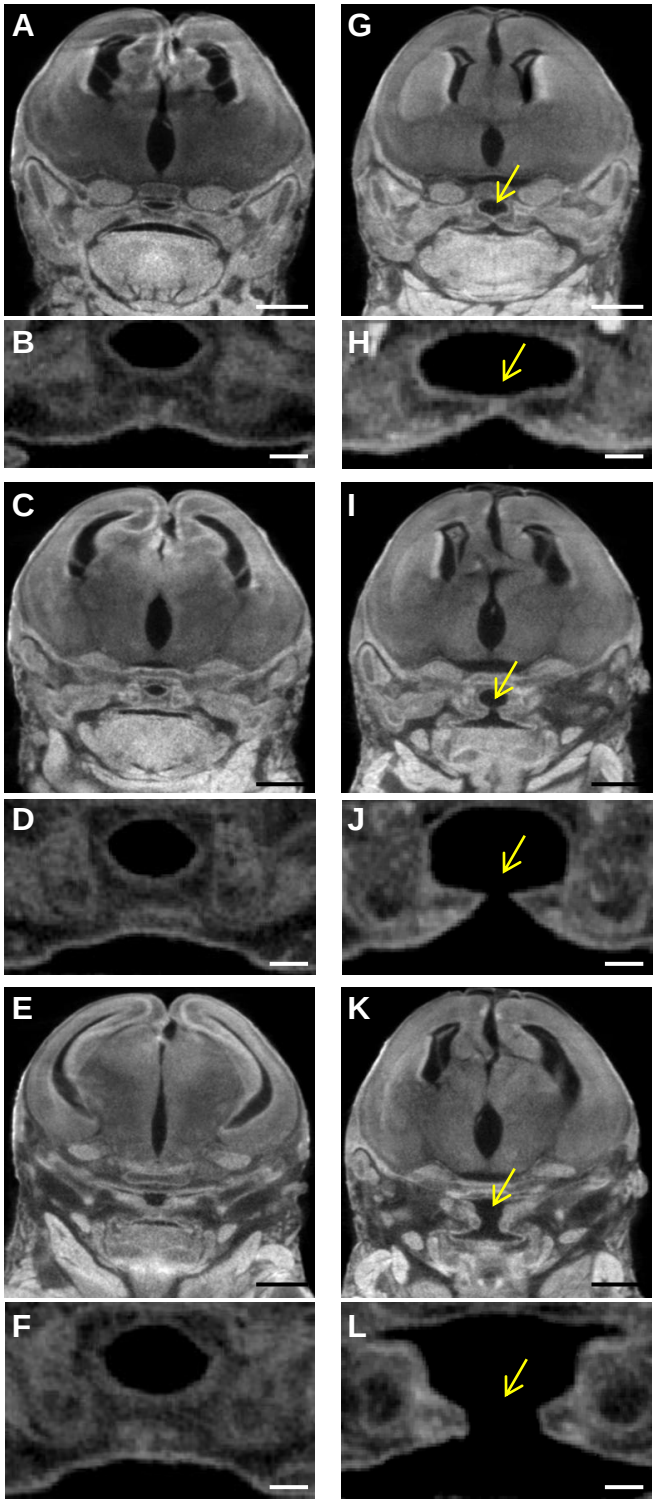

Fig. S2

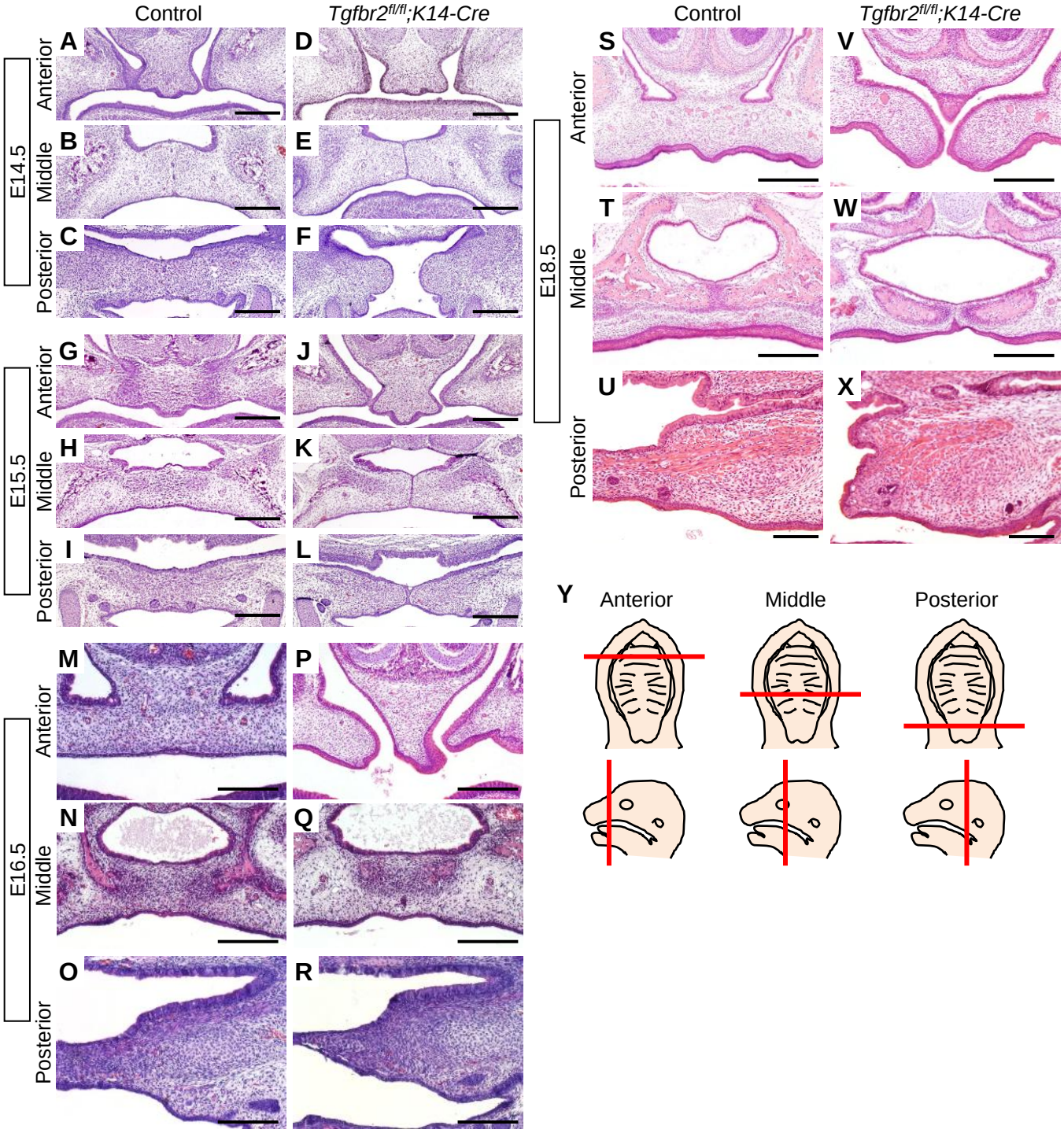
Control
Tgfbr2fl/fl;K14-Cre
Control
Tgfbr2fl/fl;K14-Cre
E14.5
E15.5
E16.5
E18.5
Anterior
Middle
Posterior
A
B
C
D
E
F
G
H
I
J
K
L
M
N
O
P
Q
R
S
T
U
V
W
X
Y
Anterior
Middle
Posterior

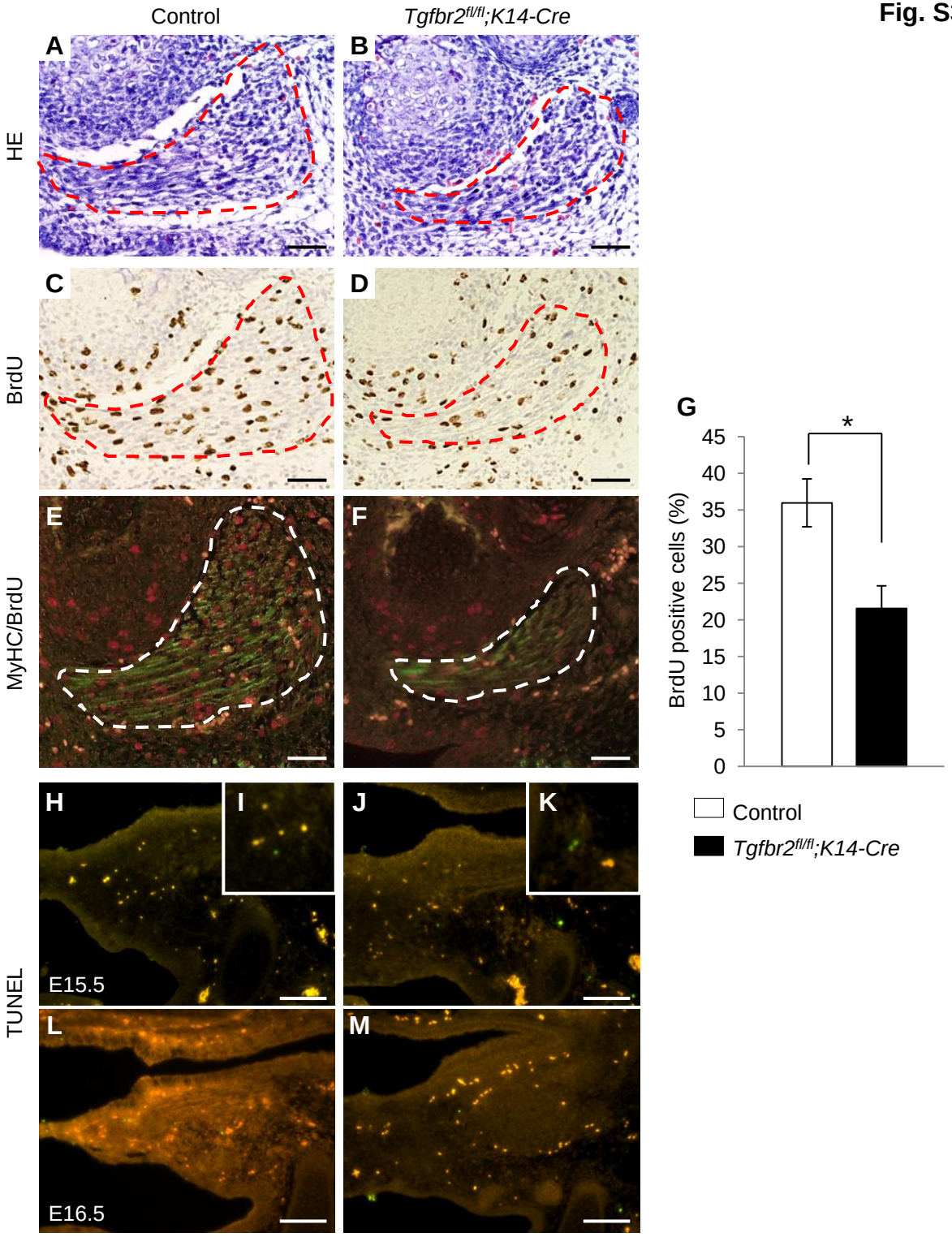
Control
Tgfbr2fl/fl;K14-Cre
A
B
HE
C
D
BrdU
E
F
MyHC/BrdU
H
I
J
K
E15.5
L
M
E16.5
TUNEL
G
BrdU positive cells (%)
45
40
35
30
25
20
15
10
5
0
*
Control
Tgfbr2fl/fl;K14-Cre

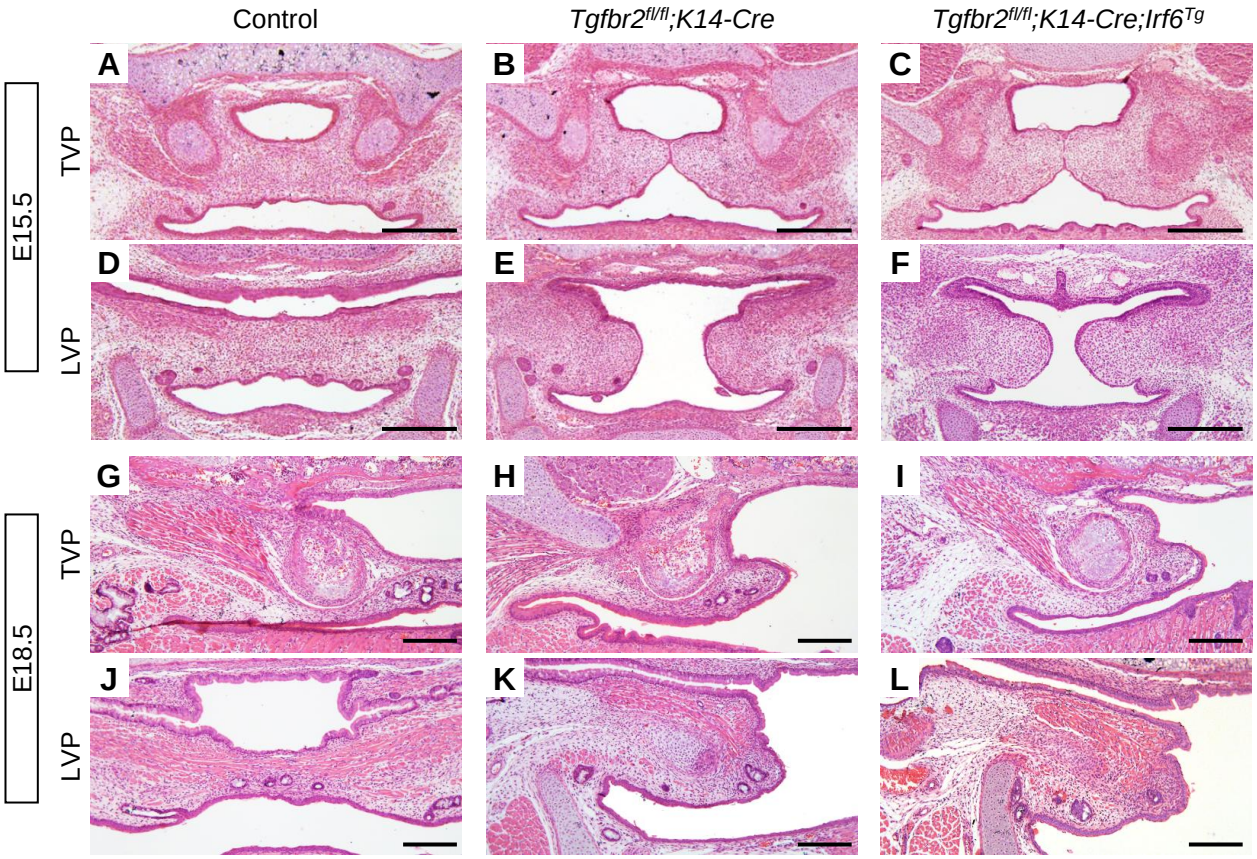
Control
Tgfbr2fl/fl;K14-Cre
Tgfbr2fl/fl;K14-Cre;Irf6Tg
E15.5
E18.5
TVP
LVP
A
B
C
D
E
F
G
H
I
J
K
L

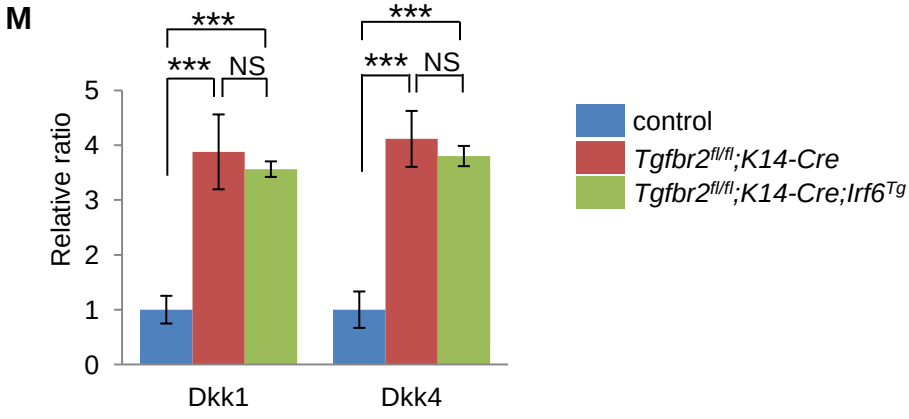
M
***
***
NS
***
***
NS
Relative ratio
0
1
2
3
4
5
Dkk1
Dkk4
control
Tgfbr2fl/fl;K14-Cre
Tgfbr2fl/fl;K14-Cre;Irf6Tg

Fig. S5

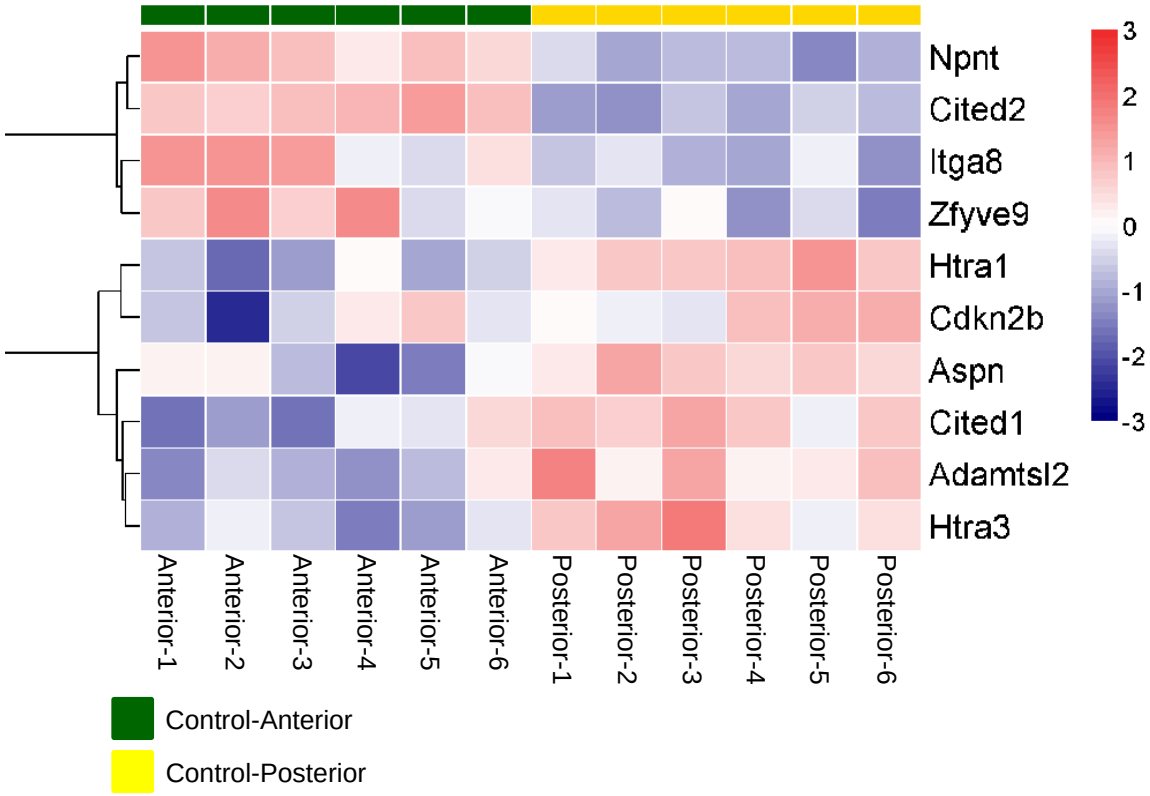
Npnt
Cited2
Itga8
Zfyve9
Htra1
Cdkn2b
Aspn
Cited1
Adamtsl2
Htra3
3
2
1
0
-1
-2
-3
Anterior-1
Anterior-2
Anterior-3
Anterior-4
Anterior-5
Anterior-6
Posterior-1
Posterior-2
Posterior-3
Posterior-4
Posterior-5
Posterior-6
Control-Anterior
Control-Posterior

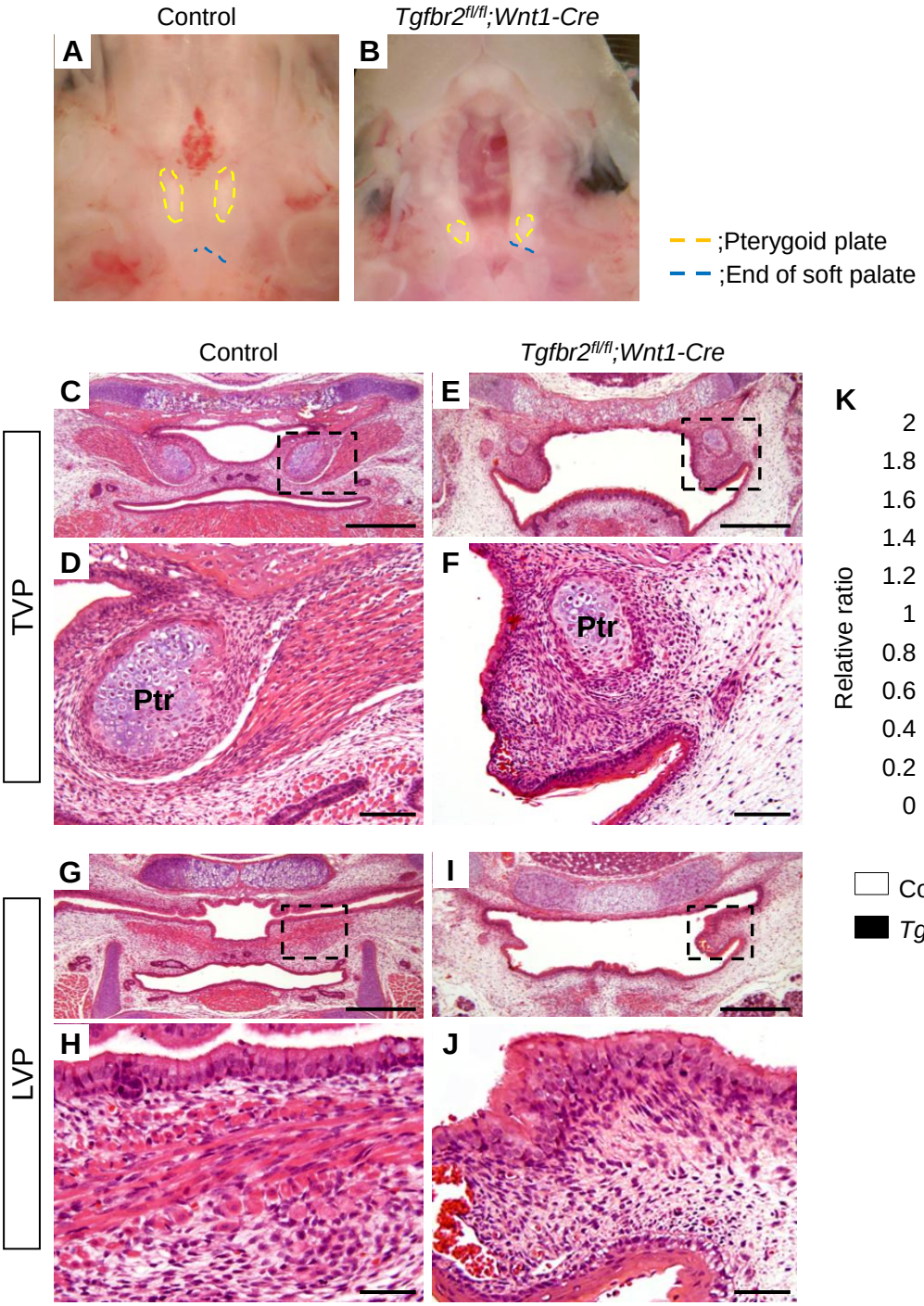
Control
Tgfbr2fl/fl;Wnt1-Cre
A
B
;Pterygoid plate
;End of soft palate
Control
Tgfbr2fl/fl;Wnt1-Cre
C
E
D
F
Ptr
Ptr
TVP
G
I
H
J
LVP
K
Relative ratio
2
1.8
1.6
1.4
1.2
1
0.8
0.6
0.4
0.2
0
*
***
Dkk2
Limd1
Control
Tgfbr2fl/fl;Wnt1-Cre

Fig. S7

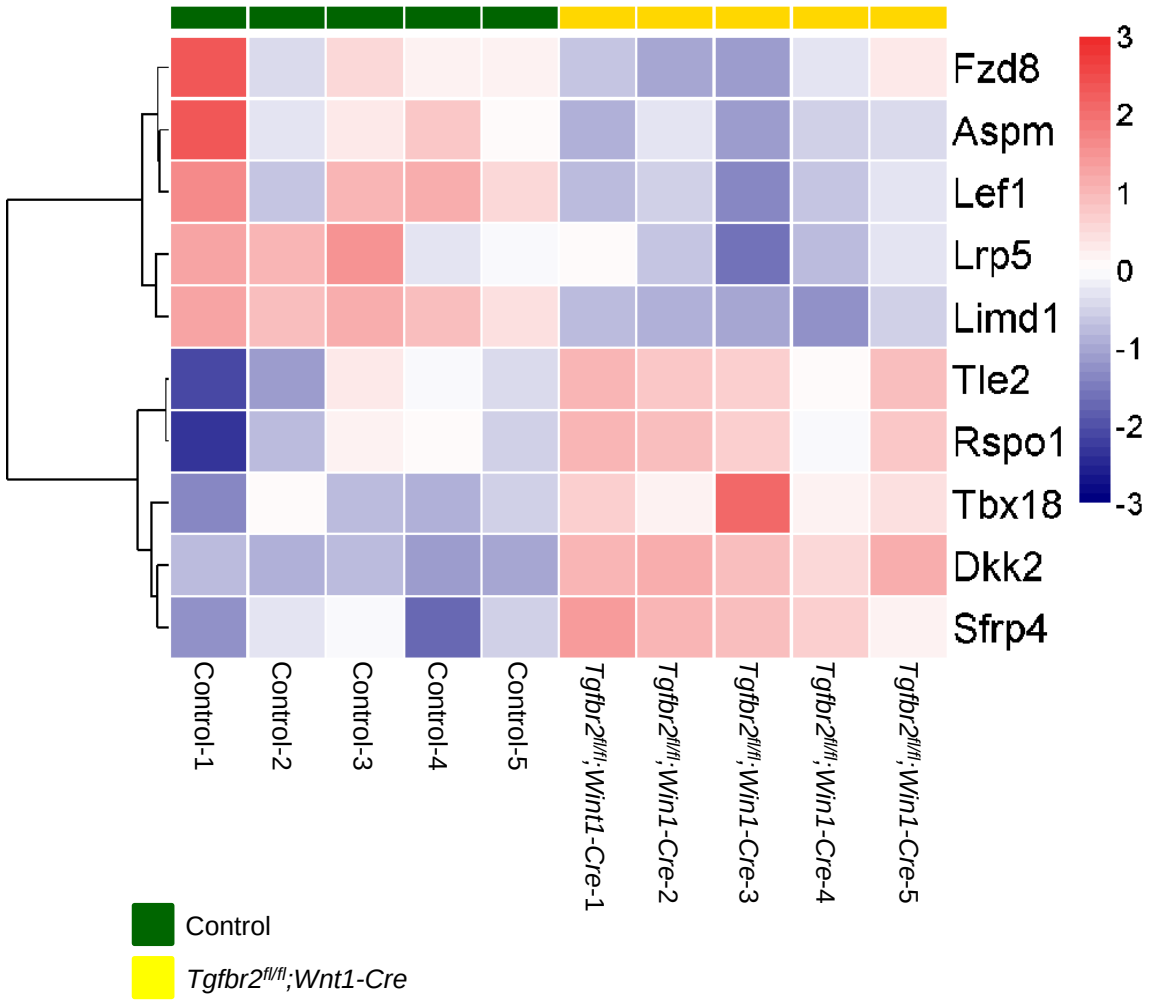
Fzd8
Aspm
Lef1
Lrp5
Limd1
Tle2
Rspo1
Tbx18
Dkk2
Sfrp4
3
2
1
0
-1
-2
-3
Control-1
Control-2
Control-3
Control-4
Control-5
Tgfbr2fl/fl;Wnt1-Cre-1
Tgfbr2fl/fl;Wnt1-Cre-2
Tgfbr2fl/fl;Wnt1-Cre-3
Tgfbr2fl/fl;Wnt1-Cre-4
Tgfbr2fl/fl;Wnt1-Cre-5
Control
Tgfbr2fl/fl;Wnt1-Cre

Supplementary Table 1. Up-regulated genes in the soft palate of *Tgfbr2*$^{fl/fl}$*;Wnt1-Cre* mice at E15.5

Probe ID	Gene Symbol	Geo Mean WT	Geo Mean Mutant	MUT POST /WT POST	FDR
1416645_a_at	Afp	9.94	448.87	45.149	0.000
1425614_x_at	H2-D1	16.98	242.07	14.256	0.000
1422588_at	Krt6b	34.18	438.47	12.829	0.001
1436879_x_at	Afp	9.13	93.19	10.203	0.000
1454608_x_at	Ttr	15.31	131.94	8.617	0.000
1443746_x_at	Dmp1	284.76	2133.51	7.492	0.008
1449133_at	Sprr1a	88.45	642.80	7.268	0.001
1455913_x_at	Ttr	11.57	80.86	6.988	0.000
1427651_x_at	H2-D1	17.11	118.96	6.951	0.000
1422253_at	Col10a1	18.99	129.91	6.842	0.037
1416646_at	Afp	28.58	191.28	6.694	0.001
1426175_a_at	Tpsab1	25.08	160.92	6.416	0.000
1449466_at	Clec3b	53.81	330.09	6.134	0.000
1443745_s_at	Dmp1	547.08	3172.86	5.800	0.031
1439483_at	AI506816	19.11	110.34	5.773	0.000
1437344_x_at	Krt13	160.11	916.35	5.723	0.006
1425447_at	Dkk4	30.67	171.78	5.602	0.010
1455848_at	Tmprss11a	65.32	354.39	5.425	0.004
1435760_at	Csta	12.43	66.08	5.318	0.000
1422454_at	Krt13	906.58	4717.33	5.203	0.005
1417614_at	Ckm	380.21	1957.40	5.148	0.015
1422401_at	Sprr3	52.63	270.32	5.136	0.000
1435761_at	BC100530	239.97	1190.49	4.961	0.013
1459737_s_at	Ttr	16.98	83.61	4.925	0.001
1429540_at	Cnfn	44.85	212.08	4.728	0.000
1430567_at	Spink5	10.72	50.66	4.727	0.000
1421979_at	Phex	164.99	777.59	4.713	0.001
1440852_at	Idi2	18.66	86.77	4.651	0.001
1452544_x_at	H2-D1	77.37	352.51	4.556	0.000
1417461_at	Cap1	414.68	1873.95	4.519	0.000
1457936_at	Mapk8	22.26	100.57	4.518	0.000
1453801_at	Them5	21.06	91.71	4.355	0.003
1451258_at	Psca	44.21	191.84	4.339	0.000
1451447_at	Cuedc1	43.16	186.89	4.330	0.000
1426005_at	Dmp1	93.77	404.75	4.316	0.012
1431035_at	Daam1	32.57	127.82	3.925	0.000
1441863_x_at	Krt13	82.94	315.29	3.801	0.039
1418735_at	Krt4	835.48	3171.82	3.796	0.002
1436329_at	Egr3	33.47	126.31	3.774	0.001
1460285_at	Itga9	88.98	325.27	3.655	0.000
1444638_at	Ttn	24.30	86.78	3.571	0.046
1437517_x_at	Serpinb3a	13.26	46.68	3.521	0.001
1438394_x_at	Krt4	1360.77	4755.36	3.495	0.001
1419527_at	Comp	41.11	143.34	3.486	0.039
1436755_at	Itih5	37.74	131.57	3.486	0.003
1450633_at	Calm4	51.19	176.82	3.454	0.003
1418511_at	Dpt	454.80	1562.51	3.436	0.002
1429159_at	Itih5	222.65	764.76	3.435	0.000
1456498_at	Itga4	20.14	68.89	3.421	0.003
1433804_at	Jak1	66.01	224.56	3.402	0.000
1419082_at	Serpinb2	21.20	70.38	3.320	0.044

Supplementary Table 1. Up-regulated genes in the soft palate of *Tgfbr2*$^{fl/fl}$*;Wnt1-Cre* mice at E15.5 (Continued)

Probe ID	Gene Symbol	Geo Mean WT	Geo Mean Mutant	MUT POST /WT POST	FDR
X00686_3_at	---	3337.28	11047.70	3.310	0.001
1449937_at	Pp11r	48.82	158.61	3.249	0.027
1417462_at	Cap1	198.94	644.81	3.241	0.000
1441946_at	Itih5	78.35	253.70	3.238	0.005
1438683_at	Wasf2	77.14	249.39	3.233	0.000
1418172_at	Hebp1	530.32	1702.26	3.210	0.000
1425538_x_at	Ceacam1	141.73	454.30	3.205	0.017
1435998_at	Ccnb1ip1	17.21	55.07	3.200	0.000
1418189_s_at	Malat1	1251.13	3997.75	3.195	0.001
1444083_at	Ttn	64.31	205.41	3.194	0.047
1445226_at	BC023969	32.06	102.14	3.186	0.000
1415931_at	Igf2	145.18	459.23	3.163	0.000
1438207_at	Gbf1	32.96	104.08	3.158	0.000
1454660_at	1100001E04Rik	133.22	420.45	3.156	0.038
1438840_x_at	Apoa1	35.55	111.07	3.125	0.009
1435639_at	2610528A11Rik	89.92	279.45	3.108	0.040
1458000_at	Dsg1a	44.86	138.95	3.098	0.013
1457266_at	---	90.45	278.96	3.084	0.000
1456120_at	Secisbp2l	40.74	125.58	3.083	0.000
1422908_at	Atp1b4	168.28	513.48	3.051	0.041
1421933_at	Cbx5	70.52	214.66	3.044	0.000
1450009_at	Ltf	94.66	287.47	3.037	0.040
1419276_at	Enpp1	27.70	83.55	3.016	0.001
1453084_s_at	Col22a1	335.23	1005.85	3.001	0.022
1449938_at	Pp11r	75.24	224.72	2.986	0.039
1435129_at	---	687.11	2049.12	2.982	0.001
1457359_at	Inpp4b	16.84	50.07	2.972	0.000
1441955_s_at	LOC676674	60.03	177.69	2.960	0.040
1440248_at	Casc4	23.79	69.99	2.942	0.003
1437127_at	A630033E08Rik	41.91	122.66	2.927	0.000
1419150_at	Myf6	57.20	167.41	2.927	0.044
1455201_x_at	Apoa1	33.33	97.24	2.918	0.003
1449894_at	Lrrc18	20.58	60.05	2.917	0.021
1418608_at	Calml3	485.22	1415.16	2.917	0.038
1426268_at	C130090K23Rik	31.42	91.45	2.911	0.000
1451999_at	Ldb3	87.15	252.99	2.903	0.045
1448469_at	Nid1	125.58	357.23	2.845	0.001
1426152_a_at	Kitl	66.32	187.82	2.832	0.008
1428301_at	100041874	260.52	735.83	2.824	0.008
1452470_at	Cep350	44.47	125.30	2.818	0.001
1422123_s_at	Ceacam1	267.60	752.61	2.812	0.015
1427797_s_at	EG665955	46.41	129.36	2.787	0.037
1450494_x_at	Ceacam1	150.93	420.46	2.786	0.026
1441125_at	Setd5	21.17	58.76	2.775	0.000
1428781_at	Dmkn	618.32	1704.69	2.757	0.041
1423594_a_at	Ednrb	93.47	257.24	2.752	0.001
1434227_at	Krtdap	615.10	1685.47	2.740	0.037
1417160_s_at	Expi	44.56	120.46	2.703	0.046
1427711_a_at	Ceacam1	20.52	55.25	2.693	0.039
1421153_at	Loxl4	53.17	143.06	2.691	0.003
1446342_at	2310001H17Rik	10.21	27.16	2.660	0.000

Supplementary Table 1. Up-regulated genes in the soft palate of *Tgfbr2*$^{fl/fl}$*;Wnt1-Cre* mice at E15.5 (Continued)

Probe ID	Gene Symbol	Geo Mean WT	Geo Mean Mutant	MUT POST /WT POST	FDR
1431281_at	Dysfip1	32.97	87.63	2.658	0.042
1418188_a_at	Malat1	667.65	1769.07	2.650	0.011
1417979_at	Tnmd	221.27	585.50	2.646	0.007
1442075_at	AI314604	36.45	96.32	2.642	0.010
1450078_at	Nrk	234.37	617.57	2.635	0.012
1423669_at	Col1a1	1881.55	4954.59	2.633	0.003
1422749_at	Ly6g6c	30.49	80.00	2.624	0.037
1425675_s_at	Ceacam1	45.58	119.11	2.613	0.039
1417814_at	Pla2g5	33.91	88.54	2.611	0.000
1427630_x_at	Ceacam1	107.88	281.00	2.605	0.030
1424808_at	Lama4	19.11	49.33	2.582	0.000
1422672_at	Sprr1b	9.26	23.90	2.580	0.024
1456088_at	Xiap	67.78	174.60	2.576	0.000
1421955_a_at	Nedd4	2204.01	5673.27	2.574	0.000
1427306_at	Ryr1	44.49	114.04	2.563	0.039
1444504_at	Dhrs7c	73.61	188.17	2.556	0.046
1443921_at	Ranbp3l	27.43	70.06	2.554	0.005
1425764_a_at	Bcat2	81.35	207.23	2.547	0.000
1440339_at	Enpp1	38.38	97.67	2.545	0.011
1421413_a_at	Pdlim5	95.05	239.49	2.520	0.040
1448228_at	Lox	1198.61	3019.95	2.520	0.006
1428909_at	A130040M12Rik	54.42	136.65	2.511	0.004
1455516_at	---	34.40	86.19	2.506	0.000
1460256_at	Car3	250.08	626.22	2.504	0.010
1448602_at	Pygm	70.13	175.53	2.503	0.041
1416930_at	Ly6d	647.24	1616.63	2.498	0.040
1443832_s_at	Sdpr	214.55	534.88	2.493	0.012
1457262_at	Smg1	58.12	144.84	2.492	0.000
1418175_at	Vdr	42.70	105.88	2.479	0.001
1448415_a_at	Sema3b	116.30	286.83	2.466	0.000
1450377_at	LOC640441	73.61	180.78	2.456	0.002
1434722_at	Ampd1	44.40	108.86	2.452	0.046
1429700_at	3110040M04Rik	13.53	33.16	2.451	0.003
1421851_at	Mtap1b	47.81	116.90	2.445	0.010
1430841_at	3300002P13Rik	34.03	83.15	2.443	0.029
1421290_at	Hspb7	29.04	70.79	2.438	0.002
1434927_at	Hspb7	30.50	74.28	2.436	0.006
1452731_x_at	100041874	158.81	386.02	2.431	0.037
1427371_at	Abca8a	166.42	401.91	2.415	0.001
1420360_at	Dkk1	209.73	506.44	2.415	0.045
1436544_at	Atp10d	110.88	267.69	2.414	0.000
1438363_at	Pnmal2	43.19	103.40	2.394	0.006
1427919_at	Srpx2	41.84	100.10	2.392	0.004
1419233_x_at	Apoa1	57.00	136.35	2.392	0.025
1450179_at	Sost	43.93	105.03	2.391	0.001
1419232_a_at	Apoa1	28.34	67.45	2.380	0.004
1422866_at	Col13a1	130.37	309.15	2.371	0.032
1451878_a_at	Jmy	16.72	39.58	2.367	0.002
1419560_at	Lipc	23.35	55.12	2.361	0.000
1417933_at	Igfbp6	46.31	108.95	2.353	0.043

Supplementary Table 1. Up-regulated genes in the soft palate of *Tgfbr2*$^{fl/fl}$*;Wnt1-Cre* mice at E15.5 (Continued)

Probe ID	Gene Symbol	Geo Mean WT	Geo Mean Mutant	MUT POST /WT POST	FDR
1455466_at	Gpr133	61.49	144.57	2.351	0.041
1423578_at	Col11a2	153.16	359.65	2.348	0.043
1419312_at	Atp2a1	211.31	495.97	2.347	0.040
1449880_s_at	Bglap-rs1	358.51	840.48	2.344	0.039
1418690_at	Ptprz1	12.93	30.23	2.337	0.002
1448367_at	Sdf4	69.84	162.91	2.333	0.000
1450051_at	Atrx	92.47	215.57	2.331	0.006
1417355_at	Peg3	1739.46	4049.63	2.328	0.001
1422546_at	Ilf3	109.77	255.46	2.327	0.000
1455593_at	Apob	14.14	32.89	2.326	0.008
1460302_at	Thbs1	254.61	591.19	2.322	0.000
1420408_a_at	Abcc9	13.41	31.10	2.318	0.009
1441384_at	Gadl1	32.06	74.17	2.313	0.003
1449862_a_at	Pi4k2b	47.72	110.02	2.305	0.042
1438588_at	Plagl1	65.30	150.42	2.303	0.007
1440150_at	Tgm3	59.79	137.64	2.302	0.005
1420097_at	D13Ertd787e	48.82	112.34	2.301	0.048
1459897_a_at	Sbsn	377.74	867.01	2.295	0.011
1450093_s_at	Zbtb7a	87.03	198.69	2.283	0.000
1459804_at	Crebbp	23.60	53.72	2.276	0.006
1430786_at	1110002E22Rik	99.86	227.28	2.276	0.048
1426498_at	Kdm5c	31.44	71.42	2.272	0.004
1437904_at	Rbm45	241.28	547.63	2.270	0.008
1436858_at	Mbnl2	168.51	381.77	2.265	0.000
1418280_at	Klf6	120.21	271.88	2.262	0.007
1443621_at	Xaf1	12.87	29.04	2.256	0.040
1447360_at	Tsc22d1	8.46	19.02	2.248	0.006
1452284_at	Ptprz1	242.38	544.68	2.247	0.000
1441111_at	---	132.26	296.37	2.241	0.047
1422481_at	Krt1	177.77	397.80	2.238	0.050
1435752_s_at	Abcc9	152.96	341.97	2.236	0.037
1416321_s_at	Prelp	48.50	108.09	2.229	0.010
1423886_at	Lamc1	58.00	129.13	2.226	0.000
1423760_at	Cd44	396.54	876.01	2.209	0.009
1436731_at	Zfp385b	108.83	239.66	2.202	0.023
1433745_at	Trio	554.71	1214.96	2.190	0.000
1427177_at	Fyco1	110.44	241.53	2.187	0.000
1425544_at	Plekha5	75.70	165.43	2.185	0.000
1427950_at	Rnf160	47.30	103.35	2.185	0.001
1418176_at	Vdr	57.82	125.61	2.172	0.000
1417552_at	Fap	371.18	805.10	2.169	0.007
1453345_at	Nipal1	49.46	106.95	2.162	0.026
1416455_a_at	Cryab	282.48	609.94	2.159	0.041
1459929_at	Zfp568	52.52	112.93	2.150	0.039
1436399_s_at	Nrk	70.13	150.75	2.150	0.037
1428662_a_at	Hopx	511.14	1096.35	2.145	0.038
1432269_a_at	Sh3kbp1	27.14	58.19	2.144	0.004
1436521_at	Slc36a2	46.92	100.55	2.143	0.010
1429357_at	Fam135a	17.05	36.49	2.141	0.000
1417626_at	Pde4dip	85.20	181.14	2.126	0.047

Supplementary Table 1. Up-regulated genes in the soft palate of *Tgfbr2*$^{fl/fl}$*;Wnt1-Cre* mice at E15.5 (Continued)

Probe ID	Gene Symbol	Geo Mean WT	Geo Mean Mutant	MUT POST /WT POST	FDR
1436037_at	Itga4	141.28	300.21	2.125	0.004
1422834_at	Kcnd2	18.43	39.16	2.125	0.030
1426285_at	Lama2	200.51	424.72	2.118	0.002
1427789_s_at	Gnas	34.04	71.91	2.113	0.012
1417956_at	Cidea	48.21	101.65	2.109	0.010
1442819_at	Rhbdl2	75.17	158.42	2.108	0.002
1449311_at	Bach1	81.79	172.32	2.107	0.000
1441333_at	---	8.22	17.29	2.104	0.026
1440879_at	Abca9	171.87	360.80	2.099	0.004
1438271_at	Lpp	43.09	90.43	2.099	0.024
1423407_a_at	Fbln2	730.79	1531.86	2.096	0.001
1416697_at	Dpp4	74.63	156.41	2.096	0.002
1431211_s_at	Them5	42.84	89.62	2.092	0.034
1449716_s_at	Nrd1	123.86	258.72	2.089	0.000
1424112_at	Igf2r	1161.71	2422.21	2.085	0.000
1460125_at	---	84.77	176.69	2.084	0.050
1439630_x_at	Sbsn	350.13	729.08	2.082	0.027
1432393_a_at	Thg1l	154.49	321.52	2.081	0.000
1420371_at	Sntb2	42.08	87.46	2.078	0.028
1419088_at	Timp3	48.12	99.83	2.074	0.000
1449434_at	Car3	1806.24	3742.59	2.072	0.040
1460426_at	Pde4dip	27.36	56.62	2.069	0.002
1451382_at	Chac1	70.37	145.59	2.069	0.014
1425218_a_at	Scgb3a2	91.29	188.87	2.069	0.000
1423065_at	Dnmt3a	282.70	584.68	2.068	0.002
1439555_at	Rlf	23.32	48.08	2.061	0.003
1449396_at	Aoc3	32.04	66.02	2.060	0.042
1429400_at	Clcn5	549.96	1131.26	2.057	0.003
1422882_at	Sypl	84.53	173.70	2.055	0.000
1429332_at	4632427E13Rik	11.42	23.39	2.049	0.004
1427019_at	Ptprz1	158.97	325.13	2.045	0.000
1456351_at	Brd8	44.60	91.20	2.045	0.000
1437536_at	Fkrp	29.29	59.70	2.039	0.003
1456537_at	A930033H14Rik	20.85	42.50	2.038	0.000
1425338_at	Plcb4	22.56	45.97	2.038	0.001
1415964_at	Scd1	179.70	366.19	2.038	0.000
1421190_at	Gabrb3	9.31	18.96	2.036	0.005
1416062_at	Tbc1d15	107.12	217.77	2.033	0.000
1450068_at	Baz1b	35.87	72.93	2.033	0.038
1434605_at	Eif5b	191.91	389.83	2.031	0.001
1420417_at	Gm2521	39.17	79.53	2.030	0.001
1449563_at	Cntn1	50.58	102.66	2.030	0.038
1437422_at	Sema5a	221.75	448.32	2.022	0.011
1456863_at	Epha4	12.11	24.45	2.019	0.002
1438667_at	5730410E15Rik	55.36	111.62	2.016	0.037
1451204_at	Scara5	148.39	298.52	2.012	0.020
1416551_at	Atp2a2	674.81	1353.21	2.005	0.017
1418403_at	Adam19	51.42	103.11	2.005	0.000
1419292_at	Htra3	266.66	534.14	2.003	0.001
1457270_at	Gas7	68.42	136.99	2.002	0.002
1419703_at	Col5a3	49.39	98.86	2.002	0.047

Supplementary Table 2. Down-regulated genes in the soft palate of *Tgfbr2*$^{fl/fl}$*;Wnt1-Cre* mice at E15.5

Probe ID	Gene Symbol	Geo Mean WT	Geo Mean Mutant	MUT POST /WT POST	FDR
1438955_x_at	Ppif	149.78	74.85	-2.001	0.001
1429222_at	Pus3	69.75	34.85	-2.001	0.007
1436726_s_at	Sptlc1	434.96	216.77	-2.007	0.044
1437132_x_at	Nedd9	680.57	338.40	-2.011	0.014
1453977_at	Exoc4	19.46	9.67	-2.013	0.000
1416886_at	C1d	190.39	94.56	-2.013	0.001
1416422_a_at	Ssb	598.06	296.29	-2.019	0.030
1416476_a_at	Ube2d2	4564.64	2251.26	-2.028	0.039
1419401_at	Asb13	67.54	33.24	-2.032	0.039
1418487_at	Ripk4	271.18	133.45	-2.032	0.017
1452713_a_at	Snrnp40	4596.19	2252.37	-2.041	0.027
1418656_at	Lsm5	3774.38	1848.42	-2.042	0.008
1429145_at	Nhlrc2	238.43	116.63	-2.044	0.037
1434578_x_at	LOC100045999	8210.53	4012.54	-2.046	0.040
1435164_s_at	Uba3	1567.23	764.50	-2.050	0.039
1423747_a_at	Pdk1	1090.85	531.76	-2.051	0.041
1436600_at	Tox3	526.01	256.40	-2.052	0.011
1425149_a_at	Pdcl	1353.03	657.97	-2.056	0.001
1459646_at	Hs3st6	204.99	99.41	-2.062	0.000
1438841_s_at	Arg2	33.18	16.05	-2.068	0.029
1438921_at	Atr	33.84	16.34	-2.071	0.000
1443153_at	Trip11	31.19	15.04	-2.073	0.000
1433568_at	Papd4	357.26	171.98	-2.077	0.017
1454951_at	Zfp606	352.63	169.62	-2.079	0.016
1441107_at	Dmrta2	755.30	363.03	-2.081	0.037
1459742_at	---	20.38	9.74	-2.094	0.000
1428162_at	4933421E11Rik	421.67	201.41	-2.094	0.004
1460244_at	Upb1	103.56	49.45	-2.094	0.001
1460399_at	Ccdc117	223.68	106.76	-2.095	0.000
1416152_a_at	Sfrs3	2665.79	1269.02	-2.101	0.009
1437914_at	E2f6	234.06	110.96	-2.109	0.000
1438349_at	Zfp229	259.13	122.78	-2.111	0.011
1434636_at	Homez	82.48	39.07	-2.111	0.028
1435252_at	B3galt6	123.88	58.65	-2.112	0.009
1429372_at	Sox11	751.69	354.20	-2.122	0.000
1455261_at	Luc7l	254.64	119.89	-2.124	0.000
1434045_at	Cdkn1b	1059.02	498.16	-2.126	0.003
1454838_s_at	Pkdcc	2387.09	1122.67	-2.126	0.018
1438659_x_at	Chchd6	1828.70	858.15	-2.131	0.006
1449482_at	Hist3h2ba	751.11	351.96	-2.134	0.039
1453136_at	Fbxo30	179.28	83.66	-2.143	0.037
1435523_s_at	2700089E24Rik	225.66	105.19	-2.145	0.040
1437490_x_at	LOC640502	407.39	189.86	-2.146	0.044
1424694_at	2010011I20Rik	202.03	93.93	-2.151	0.000
1426471_at	Zfp52	303.63	140.98	-2.154	0.000
1452593_a_at	Tceb1	206.37	95.80	-2.154	0.001
1437164_x_at	Atp5o	4214.53	1951.96	-2.159	0.023
1423422_at	Asb4	744.38	344.55	-2.160	0.007
1420726_x_at	Tmlhe	100.98	46.59	-2.167	0.032
1433757_a_at	Nisch	229.98	105.99	-2.170	0.002

Supplementary Table 2. Down-regulated genes in the soft palate of *Tgfbr2*$^{fl/fl}$*;Wnt1-Cre* mice at E15.5 (Continued)

Probe ID	Gene Symbol	Geo Mean WT	Geo Mean Mutant	MUT POST /WT POST	FDR
1428603_at	Gm16039	663.80	305.67	-2.172	0.000
1429436_at	Prpf40a	419.59	193.03	-2.174	0.008
1430135_at	Dnase2a	65.60	30.07	-2.182	0.001
1439558_at	Zfp317	122.29	56.03	-2.183	0.009
1439428_x_at	Gmds	178.21	81.64	-2.183	0.041
1440342_at	G530011O06Rik	49.96	22.87	-2.185	0.000
1460354_a_at	Mrpl13	2124.04	971.75	-2.186	0.005
1456735_x_at	Acpl2	1394.07	637.12	-2.188	0.000
1449128_at	Ccdc43	186.17	84.91	-2.193	0.027
1435532_at	LOC100048362	143.52	65.46	-2.193	0.020
1437168_at	RP23-12I24.6	156.03	71.01	-2.197	0.048
1434067_at	AI662270	105.60	47.98	-2.201	0.004
1451511_at	Hibch	85.34	38.63	-2.209	0.033
1444248_at	Rcn2	73.89	33.38	-2.213	0.000
1416267_at	Scoc	901.23	405.79	-2.221	0.041
1438511_a_at	1190002H23Rik	466.76	210.08	-2.222	0.001
1428224_at	Hnrpdl	522.25	234.68	-2.225	0.037
1422881_s_at	Sypl	1541.88	692.09	-2.228	0.044
1445274_at	Zfp781	92.39	41.46	-2.228	0.000
1430569_at	Ttc9c	97.70	43.84	-2.229	0.050
1452091_a_at	Rbm28	448.07	200.94	-2.230	0.000
1455433_at	3110048L19Rik	258.18	115.62	-2.233	0.003
1440353_at	Ntf5	394.34	176.34	-2.236	0.042
1418525_at	Pcm1	198.79	88.85	-2.237	0.002
1454842_a_at	B3galnt2	340.41	152.05	-2.239	0.012
1429335_at	Snapc1	315.36	140.75	-2.240	0.000
1418190_at	Pon1	91.34	40.72	-2.243	0.007
1425495_at	Zfp62	286.18	127.48	-2.245	0.044
1435435_at	Cttnbp2	145.71	64.83	-2.248	0.001
1460218_at	Cd52	419.37	186.20	-2.252	0.000
1451181_at	Tmem121	360.94	159.95	-2.257	0.000
1441890_x_at	Tmeff1	172.27	76.25	-2.259	0.024
1429490_at	Rif1	245.85	108.26	-2.271	0.012
1439475_at	Zfp429	131.73	57.94	-2.274	0.000
1423804_a_at	Idi1	535.69	235.11	-2.279	0.030
1441941_x_at	Serpinb5	526.83	231.06	-2.280	0.047
1456736_x_at	Mff	3806.07	1666.54	-2.284	0.001
1428304_at	Esco2	251.37	110.00	-2.285	0.031
1440125_at	A530054K11Rik	42.90	18.65	-2.300	0.008
1434014_at	Atg4c	228.01	99.07	-2.301	0.000
1452426_x_at	---	18.15	7.88	-2.304	0.000
1437286_x_at	1110020G09Rik	91.25	39.55	-2.307	0.042
1454885_at	BC063263	130.14	56.38	-2.308	0.001
1418138_at	Sult1d1	25.77	11.14	-2.314	0.000
1448609_at	Tst	1326.02	572.34	-2.317	0.040
1436684_a_at	Riok2	605.18	261.05	-2.318	0.001
1453070_at	Pcdh17	267.68	114.84	-2.331	0.042
1456698_s_at	Hnrpdl	2775.18	1189.48	-2.333	0.039
1441797_at	---	45.26	19.32	-2.342	0.005
1456244_x_at	Glrx3	3061.48	1305.02	-2.346	0.002

Supplementary Table 2. Down-regulated genes in the soft palate of *Tgfbr2*$^{fl/fl}$*;Wnt1-Cre* mice at E15.5 (Continued)

Probe ID	Gene Symbol	Geo Mean WT	Geo Mean Mutant	MUT POST /WT POST	FDR
1455883_a_at	Lrrtm1	861.38	366.58	-2.350	0.042
1416179_a_at	Rdx	3278.56	1393.00	-2.354	0.048
1433866_x_at	Prdx1	7822.40	3323.55	-2.354	0.044
1447202_at	1200009F10Rik	110.23	46.81	-2.355	0.000
1424409_at	Cldn23	646.43	274.17	-2.358	0.043
1457278_at	6720489N17Rik	48.87	20.73	-2.358	0.000
1454402_at	3110048L19Rik	16.16	6.85	-2.358	0.001
1451931_x_at	H2-L	618.59	262.19	-2.359	0.010
1430357_at	H3f3b	260.50	110.39	-2.360	0.024
1453749_at	2610507I01Rik	92.48	39.18	-2.361	0.001
1435471_at	Zfp708	127.00	53.74	-2.363	0.000
1449152_at	Cdkn2b	204.15	86.37	-2.364	0.005
1447977_x_at	3100002L24Rik	272.29	115.01	-2.368	0.001
1424264_at	Med6	528.68	223.24	-2.368	0.022
1429285_at	Serpina9	95.28	40.19	-2.371	0.038
1438487_s_at	Zzz3	485.96	204.73	-2.374	0.044
1418428_at	Kif5b	1080.43	454.94	-2.375	0.046
1438455_at	Pabpc4l	335.48	141.13	-2.377	0.040
1447825_x_at	Pcdh8	301.33	126.68	-2.379	0.005
1437711_x_at	Gm6742	3135.44	1317.05	-2.381	0.049
1450140_a_at	Cdkn2a	32.96	13.72	-2.402	0.001
1437461_s_at	Rnpc3	521.14	215.89	-2.414	0.001
1450896_at	Arhgap5	478.50	197.91	-2.418	0.039
1438786_a_at	2610021A01Rik	252.83	104.56	-2.418	0.011
1426593_a_at	Fbxo22	1295.73	534.25	-2.425	0.039
1417208_at	Amacr	428.89	176.08	-2.436	0.000
1428586_at	Tmem41b	236.23	96.63	-2.445	0.042
1453245_at	9130024F11Rik	117.56	47.84	-2.458	0.000
1453040_at	Mcart6	195.08	79.33	-2.459	0.000
1423487_at	Cript	27.81	11.31	-2.459	0.000
1418499_a_at	Kcne3	496.40	201.21	-2.467	0.000
1426243_at	Cth	279.81	113.40	-2.467	0.000
1454642_a_at	Commd3	1880.03	761.69	-2.468	0.038
1438754_at	---	50.90	20.56	-2.475	0.001
1457044_at	Macc1	172.56	69.41	-2.486	0.006
1454701_at	4930503L19Rik	138.52	55.53	-2.494	0.040
1437152_at	Mex3b	1512.21	605.64	-2.497	0.038
1436981_a_at	Ywhaz	646.91	259.06	-2.497	0.039
1423832_at	Prkag2	106.59	42.58	-2.503	0.003
1451065_a_at	Ddx39	2234.19	891.38	-2.506	0.020
1438984_x_at	Psmb4	5731.91	2281.86	-2.512	0.042
1437911_at	6330416L07Rik	147.37	58.66	-2.512	0.000
1447837_x_at	Polh	535.60	213.09	-2.513	0.005
1425315_at	Dock7	53.18	21.10	-2.520	0.001
1416826_a_at	Med20	879.44	346.86	-2.535	0.000
1453568_at	Dapl1	917.86	361.88	-2.536	0.015
1428375_at	4932415G12Rik	111.20	43.83	-2.537	0.000
1452348_s_at	Gm2785	57.55	22.68	-2.538	0.008
1437285_at	1110020G09Rik	73.00	28.73	-2.540	0.024
1447703_x_at	Zfp593	688.95	270.23	-2.549	0.000

Supplementary Table 2. Down-regulated genes in the soft palate of *Tgfbr2*$^{fl/fl}$*;Wnt1-Cre* mice at E15.5 (Continued)

Probe ID	Gene Symbol	Geo Mean WT	Geo Mean Mutant	MUT POST /WT POST	FDR
1454898_s_at	Iah1	776.86	304.24	-2.553	0.010
1425646_at	BC016495	62.76	24.51	-2.560	0.000
1423792_a_at	Cmtm6	450.31	175.70	-2.563	0.046
1452876_x_at	2610044O15Rik	167.59	64.91	-2.582	0.004
1424292_at	Depdc1a	547.72	211.48	-2.590	0.002
1456032_x_at	Gm8203	4913.88	1896.96	-2.590	0.039
1436330_x_at	Gm7072	229.29	87.12	-2.632	0.000
1439442_x_at	Yars2	329.23	125.07	-2.632	0.005
1451683_x_at	H2-D1	81.72	30.98	-2.638	0.000
1448716_at	Hba-x	504.97	190.72	-2.648	0.012
1416290_a_at	Psmc4	4243.79	1602.07	-2.649	0.024
1436390_a_at	Clcc1	508.30	191.33	-2.657	0.041
1420725_at	Tmlhe	120.72	45.36	-2.661	0.009
1423142_a_at	Gtpbp4	704.05	263.93	-2.668	0.040
1433453_a_at	Abtb2	515.24	192.19	-2.681	0.039
1455384_x_at	D030056L22Rik	607.57	226.24	-2.686	0.000
1438922_x_at	Gm5256	1275.03	468.95	-2.719	0.014
1450717_at	Ang	92.82	34.10	-2.722	0.000
1458667_at	Ninl	40.83	14.98	-2.726	0.022
1435661_at	Als2cr4	808.81	295.86	-2.734	0.045
1428693_at	2610044O15Rik	181.56	66.25	-2.741	0.002
1444589_at	Gm4944	136.37	49.74	-2.742	0.000
1429007_at	Slc35b2	163.69	59.22	-2.764	0.000
1452083_a_at	Pja1	760.74	275.14	-2.765	0.039
1439406_x_at	Fars2	166.66	60.26	-2.766	0.018
1456862_at	Six4	332.30	119.39	-2.783	0.043
1428490_at	C1galt1	407.23	146.15	-2.786	0.001
1431708_a_at	Tia1	149.23	52.94	-2.819	0.014
1417845_at	Cldn6	558.47	197.65	-2.826	0.009
1439753_x_at	Six4	329.77	116.63	-2.828	0.047
1423640_at	Synpr	206.45	72.96	-2.830	0.001
1428738_a_at	D14Ertd449e	2276.36	797.75	-2.853	0.000
1431225_at	---	690.79	242.01	-2.854	0.007
1425545_x_at	H2-D1	722.88	252.52	-2.863	0.045
1434150_a_at	Higd1c	826.16	286.31	-2.886	0.008
1455213_at	Tmsb15b1-Tmsb15b2	1388.94	476.22	-2.917	0.000
1438360_x_at	Gm5256	1499.51	513.93	-2.918	0.021
1456746_a_at	Cd99l2	231.46	79.28	-2.919	0.038
1435682_at	Lars2	364.83	124.39	-2.933	0.000
1437987_at	---	89.93	30.59	-2.939	0.000
1434236_at	Zdhhc20	594.25	199.93	-2.972	0.039
1455648_at	---	293.40	98.05	-2.992	0.000
1451784_x_at	H2-D1	706.03	234.49	-3.011	0.042
1460434_at	Fundc2	302.14	100.27	-3.013	0.000
1456467_s_at	Nlk	145.68	48.28	-3.018	0.019
1422606_at	C1qtnf3	784.46	259.58	-3.022	0.042
1448872_at	Reg3g	744.31	245.36	-3.034	0.038
1437313_x_at	Hmgb2	4118.52	1355.14	-3.039	0.041
1420622_a_at	Hspa8	7052.32	2318.07	-3.042	0.039
1416166_a_at	Prdx4	2313.23	756.27	-3.059	0.040

Supplementary Table 2. Down-regulated genes in the soft palate of *Tgfbr2*$^{fl/fl}$*;Wnt1-Cre* mice at E15.5 (Continued)

Probe ID	Gene Symbol	Geo Mean WT	Geo Mean Mutant	MUT POST /WT POST	FDR
1456097_a_at	Itgb3bp	398.91	130.36	-3.060	0.000
1431686_a_at	Gmfb	147.67	47.84	-3.087	0.000
1436298_x_at	Paics	2290.72	732.79	-3.126	0.050
1449153_at	Mmp12	112.92	36.00	-3.137	0.021
1435370_a_at	Ces3	193.32	61.61	-3.138	0.009
1438758_at	Adi1	599.72	191.02	-3.140	0.000
1419453_at	Uchl5	36.92	11.71	-3.152	0.000
1427151_at	Qser1	227.94	72.19	-3.158	0.049
1437172_x_at	Hadhb	1823.31	575.36	-3.169	0.047
1434700_at	G2e3	156.28	49.23	-3.175	0.000
1428414_at	Ccny	206.58	64.91	-3.182	0.000
1417222_a_at	Tmem123	1657.00	509.39	-3.253	0.048
1452473_at	Prr15	536.93	164.81	-3.258	0.020
1424573_at	Tmed5	912.33	277.63	-3.286	0.041
1425926_a_at	Otx2	162.01	49.09	-3.300	0.021
1429527_a_at	Plscr1	487.60	146.57	-3.327	0.008
1423436_at	Gsta3	613.77	183.26	-3.349	0.041
1453985_at	0610007P08Rik	77.55	23.11	-3.355	0.000
1451190_a_at	Sbk1	2057.35	612.96	-3.356	0.019
1454725_at	Tra2a	2486.09	734.41	-3.385	0.012
1437995_x_at	7-Sep	3904.94	1153.42	-3.386	0.040
1417769_at	Psmc6	301.35	88.47	-3.406	0.013
1459714_at	---	63.37	18.51	-3.424	0.000
1418940_at	Sult1b1	108.15	31.51	-3.432	0.000
1422916_at	Fgf21	130.80	38.00	-3.442	0.000
1417408_at	F3	1362.93	389.93	-3.495	0.043
1416911_a_at	Akirin1	1372.78	392.03	-3.502	0.039
1447868_x_at	Glrx3	204.34	58.33	-3.503	0.002
1455292_x_at	Rsl1	258.81	73.82	-3.506	0.000
1435884_at	Itsn1	286.63	81.00	-3.539	0.043
1421144_at	Rpgrip1	533.11	150.06	-3.553	0.000
1456532_at	Pdgfd	202.55	56.92	-3.558	0.016
1417051_at	Pcdh8	256.02	71.00	-3.606	0.000
1417069_a_at	Gmfb	354.91	98.04	-3.620	0.000
AFFX-DapX-3_at	---	6325.54	1714.60	-3.689	0.000
1429712_at	Gm14288	1108.28	297.76	-3.722	0.000
AFFX-ThrX-3_at	---	1576.30	420.50	-3.749	0.003
1430979_a_at	Prdx2	2061.53	540.40	-3.815	0.000
1460628_at	Eme2	53.14	13.93	-3.815	0.000
AFFX-r2-Bs-dap-3_at	---	6912.36	1811.01	-3.817	0.000
1457588_at	C76213	70.16	18.27	-3.840	0.000
AFFX-r2-Bs-thr-3_s_at	---	2235.19	578.84	-3.862	0.001
1437850_a_at	Cnbp	3296.98	849.45	-3.881	0.043
1460713_at	BC048355	478.54	122.88	-3.894	0.000
1459835_s_at	Dnaja1	1862.60	473.10	-3.937	0.039
1435702_s_at	Ywhae	2675.97	679.09	-3.940	0.033
AFFX-DapX-M_at	---	4183.48	1054.96	-3.966	0.000
1434452_x_at	Eif2a	855.86	215.53	-3.971	0.041

Supplementary Table 2. Down-regulated genes in the soft palate of *Tgfbr2*$^{fl/fl}$*;Wnt1-Cre* mice at E15.5 (Continued)

Probe ID	Gene Symbol	Geo Mean WT	Geo Mean Mutant	MUT POST /WT POST	FDR
AFFX-r2-Bs-thr-M_s_at	---	1126.88	276.39	-4.077	0.002
1429691_at	Ptprg	376.57	90.80	-4.147	0.000
AFFX-PheX-3_at	---	872.55	206.92	-4.217	0.001
AFFX-r2-Bs-dap-M_at	---	4504.20	1052.55	-4.279	0.000
AFFX-ThrX-5_at	---	593.43	129.78	-4.572	0.007
1457352_x_at	Svopl	95.99	20.80	-4.615	0.000
AFFX-r2-Bs-thr-5_s_at	---	631.82	134.39	-4.702	0.011
1437502_x_at	Cd24a	3584.35	762.00	-4.704	0.044
1417797_a_at	1810019J16Rik	504.94	106.61	-4.736	0.001
1416187_s_at	Pnrc2	3101.09	633.71	-4.894	0.040
AFFX-ThrX-M_at	---	836.86	169.63	-4.933	0.001
1439059_at	BC031748	136.24	27.49	-4.957	0.007
AFFX-r2-Bs-dap-5_at	---	2362.96	476.40	-4.960	0.003
1449033_at	Tnfrsf11b	180.27	36.30	-4.966	0.009
1460668_at	Gal	987.26	194.42	-5.078	0.001
1437128_a_at	A630033E08Rik	97.35	19.03	-5.116	0.000
1439780_at	Rpl7l1	230.12	44.84	-5.131	0.001
AFFX-r2-Bs-phe-3_at	---	1213.76	235.88	-5.146	0.000
1456688_at	---	55.99	10.82	-5.174	0.000
AFFX-DapX-5_at	---	1746.51	334.87	-5.215	0.002
1448973_at	Sult1d1	93.95	17.69	-5.311	0.000
1437726_x_at	C1qb	902.07	165.92	-5.437	0.000
AFFX-LysX-3_at	---	1167.31	212.73	-5.487	0.000
AFFX-LysX-M_at	---	587.92	103.49	-5.681	0.000
AFFX-PheX-M_at	---	835.21	144.51	-5.780	0.000
1439415_x_at	Gm5963	1162.09	200.25	-5.803	0.040
1437262_x_at	Bcas2	329.20	56.34	-5.843	0.031
1422716_a_at	Acp1	580.72	97.23	-5.972	0.038
1436107_at	Lsm8	122.19	19.16	-6.379	0.000
AFFX-r2-Bs-lys-3_at	---	535.14	83.66	-6.397	0.000
1447831_s_at	Mtmr7	133.12	20.75	-6.416	0.000
1438238_at	2010315B03Rik	184.53	27.73	-6.655	0.000
AFFX-r2-Bs-phe-M_at	---	1073.56	157.93	-6.798	0.000
AFFX-r2-Bs-lys-5_at	---	599.70	83.29	-7.200	0.000
1434171_at	Zfp874	177.10	24.53	-7.219	0.000
AFFX-r2-Bs-lys-M_at	---	627.02	86.64	-7.237	0.000
AFFX-PheX-5_at	---	719.05	95.45	-7.534	0.000
1438936_s_at	Ang	614.05	80.75	-7.605	0.001
1436717_x_at	Hbb-y	8663.57	1132.87	-7.647	0.000
AFFX-r2-Bs-phe-5_at	---	1193.76	153.75	-7.764	0.000
1436823_x_at	Hbb-y	8727.03	1117.78	-7.807	0.000
1423696_a_at	Psmd6	3460.08	418.31	-8.272	0.000
1434280_at	---	1007.31	121.60	-8.284	0.000
1450621_a_at	Hbb-y	3818.24	459.11	-8.317	0.000
AFFX-LysX-5_at	---	411.97	48.75	-8.450	0.000
1438937_x_at	Ang	238.65	27.81	-8.582	0.000
1435514_at	Lztfl1	110.14	10.97	-10.041	0.000
1452239_at	Gt(ROSA)26Sor	359.15	28.96	-12.400	0.000